neovascularization and disturbed restoration of blood flow to ischemic limbs, suggesting that CXCR4 is important for therapeutic integration of EPC into the vascular bed [21].

Based on the above concerns and the mechanistic findings, we sought to identify a functional mouse EPC population via enhanced homing mechanism. In pursuit of this goal, we analyzed the EPC properties of mouse bone marrow derived c-Kit$^+$/Sca-1$^+$/Lin$^-$ cells (KSL), c-kit$^+$/Lin$^-$ cells (KL), Sca-1$^+$/Lin$^-$ cells (SL) and together with CD34$^+$ cells. Our results suggest that mouse CD34$^+$ cells may represent a functional EPC population in mouse bone marrow.

Results

Population of KSL, KL, SL and CD34$^+$ cells

Initially we determined the populations to investigate. For KL, SL and KSL cell isolation, lineage positive cells, counting about 90%, were depleted from total BMMNCs. KL cells and SL cells counted 37.37±0.04% and 13.27±0.01% respectively in lineage negative BMMNCs. KSL cells were included in KL or SL cells, and counted 5.97±0.01% in lineage negative BMMNCs. For CD34$^+$ cell isolation, CD34$^+$ cells were 12.23±0.02% in total BMMNCs (Figure 1a). The levels of expression of CD34 by KSL, KL and SL cells are 89.8%, 72% and 55.9%, respectively (Figure S1).

In summary, c-Kit$^+$/Lin$^-$ (KL, 3.737±0.004%) cells, Sca-1$^+$/Lin$^-$ (SL, 1.327±0.001%) cells, Sca-1$^+$/c-Kit$^+$/Lin$^-$ (KSL, 0.597±0.001%) cells and CD34$^+$ cells (12.23±0.02%) were isolated from mouse total BMMNCs by FACS.

Low colony forming activity in CD34$^+$ cells

First, we evaluated the EPC colony forming capacities of KSL, KL, SL and CD34$^+$ cells as described before [16,22]. An EPC-colony forming assay (CFA) was recently established in our laboratory. EPCs can form two types of EPC colony clusters, small (primitive) and large (definitive) EPC colonies. Small EPC colonies contain mainly small and round cells, whereas large EPC colonies are composed of large and spindle-shaped cells (Figure 1c). Both colony types are positive for the uptake of Ac-LDL and for labeling with an EC-specific marker, isolectin B4 (Figure 1d). In the current study, KSL cells had the highest capacity to form both large and small colonies (small colonies: 34±7/500 cells, large colonies: 16±3/500 cells) (Figure 1b). KL (small colonies: 8±2/500 cells, large colonies: 6±2/500 cells) and SL cells (small colonies: 13±4/500 cells, large colonies: 6±3/500 cells) formed fewer colonies than KSL cells but still overall more colonies than CD34$^+$ cells.

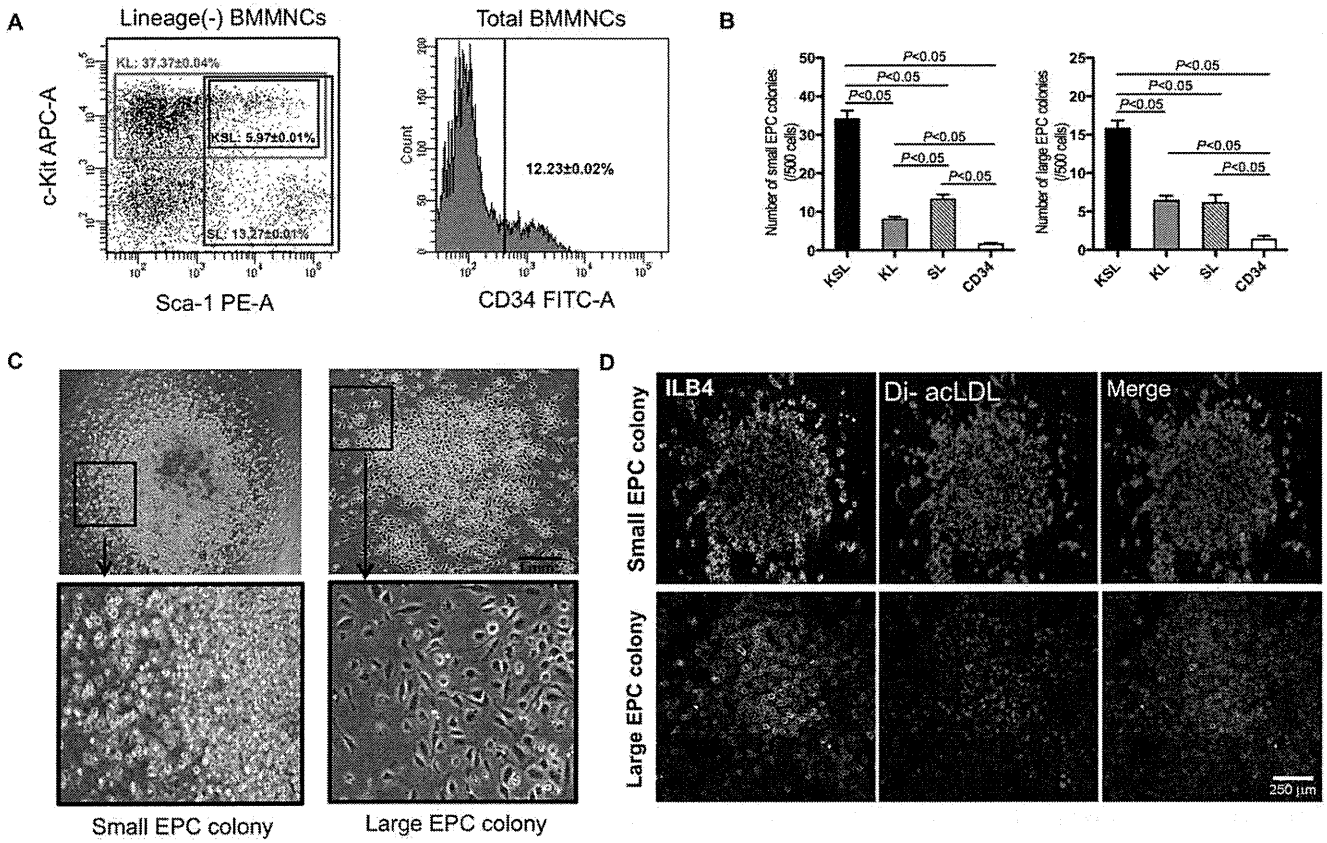

Figure 1. Isolation of KSL, KL, SL, and CD34$^+$ cells by FACS and EPC-CFA. a, Lineage depleted BMMNCs were stained with APC anti-c-kit and PE anti-Sca-1 antibodies followed by FACS sorting. The cell fractions gated with black, red, and blue frames were defined as KSL, KL, and SL cells, respectively. Also BMMNCs were stained with a FITC anti-CD34 antibody followed by FACS sorting for CD34 positive cells. b, The number of colonies was counted in each group. Small EPC colony count in each group and large EPC colony count in each group. c, EPC-CFA was performed with KSL, KL, SL, and CD34$^+$ cells, and the morphologies of small EPC colony and large EPC colony were dispalyed. The framed areas were magnified in lower panels. d, Representative double staining for Fluorescein isolectin B4 (ILB4) and DiI-acLDL in KSL cell-formed colonies. All assays were triplicated and demonstrated similar results.
doi:10.1371/journal.pone.0020219.g001

CD34$^+$ cells showed the lowest colony forming capacity (small colonies: 2±1/500 cells, large colonies: 1±1/500 cells) (Figure 1b).

Phenotypes of large and small EPC colonies

Small and large EPC colonies were collected separately after 7 days culture in methylcellulose medium. The phenotypes were analyzed by flow cytometry. The positive percentages of VE-cadherin, Flk-1 and Tie-2 were 5.3%, 3.7%, 2.9% in large colonies, respectively, 5.1%, 0.5%, 0.3% in small colonies, respectively (Figure S2a and S2b); while the positive percentages of c-Kit and Sca-1 were 4.8%, 4.4% in large colonies, respectively, 9.2%, 13.1% in small colonies, respectively (Figure S2a and S2b), which indicates that large colonies are more differentiated than small colonies. The positive percentages of CD19, CD3, CD14, CD41 and CD45 were 2.5%, 3.2%, 1.4%, 7.5%, 99.9% in large colonies, respectively, 0.1%, 0.2%, 0.3%, 9.1%, 100% in small colonies, respectively (Figure S2a and S2b).

Enhanced endothelial phenotype of CD34$^+$ cells following an adhesive culture assay

The cell culture assay was performed to further characterize all cell populations. Cells were cultured in differentiation medium for 7 days. CD34$^+$ (172±19 cells/mm^2) and KL cells (179±28 cells/mm^2) showed more numbers of adherent cells than KSL (133±38 cells/mm^2) and SL cells (128±19 cells/mm^2) ($P<0.05$, CD34 vs SL; $P<0.05$, KL vs KSL and SL) (Figure 2a and 2b).

The expression of endothelial markers in cultured KSL, KL, SL, and CD34$^+$ cells was assessed by fluorescent immunocytochemical staining and real-time RT-PCR. Consistent with the previous report that cultured EPCs express endothelial markers such as VE-cadherin, vWF and Flk-1 [23], a significant number of cells expressed VE-cadherin, vWF and Flk-1 protein in each group (Figure 3a). RT-PCR revealed that at day three CD34$^+$ cells had the highest mRNA expression levels of VE-cadherin, Flk-1 and vWF (Figure 3b). While all the cells before culture expressed low and similar levels of these markers (data not shown).

Higher angiogenic capacity in CD34$^+$ cells in vitro

The in vitro incorporation capacity of the cells was assayed via a previously described tube formation assay system [24]. HUVECs were employed to form tube-like structures. KSL, KL, SL and CD34$^+$ cells were seeded together with HUVECs, incorporating into tube-like structures and supporting their growth. One thousand (1,000) DiI-labeled cells and 12,500 HUVECs were seeded onto Matrigel-coated 96 well plates. After 24 hours in culture, incorporation of each cell population into tube-like structures formed by HUVECs was evaluated under fluorescence microscopy. Augmented cell incorporation was found for the CD34$^+$, KSL and KL groups compared to the SL group (CD34: 16±3, KSL: 13±2, KL: 15±2, SL: 8±2; $P<0.05$, SL vs CD34, KL and KSL) (Figure 4a and 4b).

Higher recruitment capacity of CD34$^+$ cells in vitro and in vivo

Next, we examined the homing capacity of these cells in mouse MI models. For tracking the fate of grafted EPCs in mouse myocardium, transplanted cells were labeled with CM-DiI after isolation by FACS and then delivered systemically three days after MI induction. Heart samples harvested one day after cell injection and examined for the presence of fluorescent-labeled cells. DiI-positive cells were observed in the infarcted myocardium of all examined groups (Figure 5a). However, the most dramatic immediate cell recruitment to ischemic myocardium was detected in the CD34$^+$ cell-injected group (CD34: 112±41/mm^2, KSL: 74±34/mm^2, KL: 47±21/mm^2 and SL: 57±24/mm^2; $P<0.05$, CD34 vs KSL, KL and SL) (Figure 5b). No significant differences among the numbers of recruited cells in the KSL, KL and SL groups could be observed. Integrin β2 has been reported previously to be critical adhesion molecules for the homing of EPCs to ischemic tissue [18,19,20,25]. SDF1/CXCR4 axis has also been shown to be one of the major chemokine/receptor signalings for EPC recruitment [26,27,28]. CXCR4 is also crucial for homing of transplanted EPC into ischemic tissues [21]. We thus assessed the mRNA expression levels of these homing-related molecules in the cells that were used for transplantation. We observed a marked up-regulation of integrin β2 and CXCR4 in CD34$^+$ cells (Figure 5c and 5d). KL cells also exhibited higher expression levels of CXCR4 (Figure 5d).

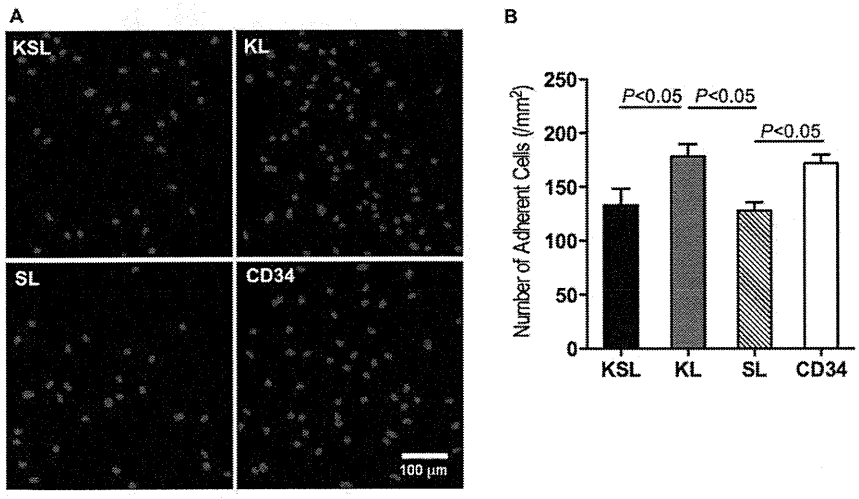

Figure 2. Culture assay with KSL, KL, SL, and CD34$^+$ cells. Freshly isolated KSL, KL, SL, and CD34$^+$ cells were cultured in 20%FBS/EGM-2MV medium on vitronectin-coated 4 well-chamber slides for 7 days. a, The cells were washed by PBS for three times and stained with DAPI. b, The numbers of adherent cells were counted and analyzed (n = 3). The assay was triplicated and demonstrated similar results.
doi:10.1371/journal.pone.0020219.g002

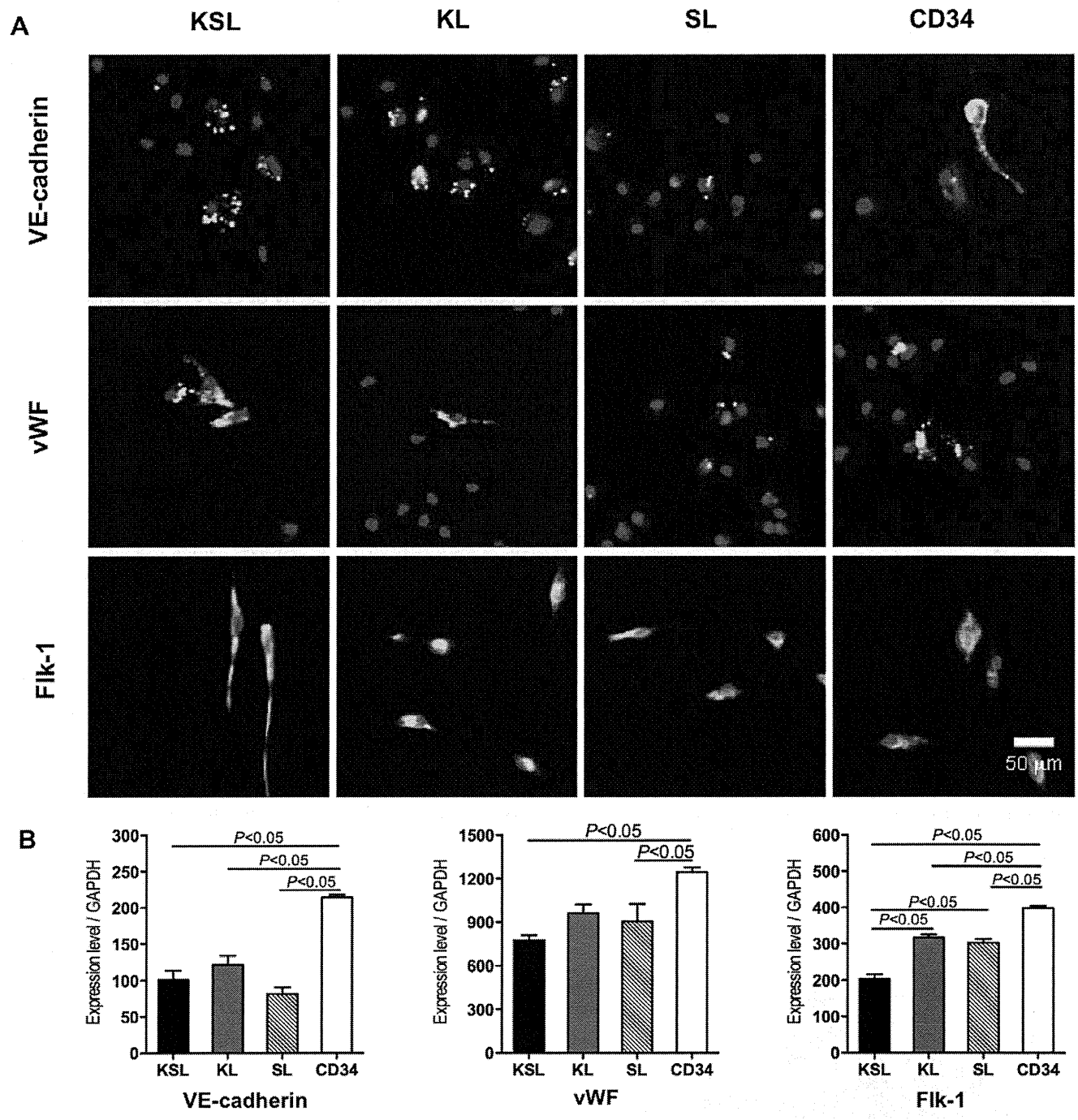

Figure 3. Assessment of endothelial markers in cultured KSL, KL, SL, and CD34$^+$ cells by immunocytostaining and real-time RT-PCR. Freshly isolated cells were cultured in 20%FBS/EGM-2MV medium on vitronectin-coated 4 well-chamber slides for 7 days. a, Adherent cells were stained with endothelial markers, VE-cadherin, vWF, and Flk-1. b, mRNA expression levels of the markers in 3-days cultured cells were assessed by quantitative real-time RT-PCR. The mRNA expressions were normalized to GAPDH (n = 3). All assays were triplicated and demonstrated similar results.
doi:10.1371/journal.pone.0020219.g003

Enhanced cell retention, vasculogenic activity and reduced fibrosis in ischemic hearts by CD34$^+$ transplantation

To track the injected cells in vivo for 28 days, we employed cells, isolated from ROSA mice, that constitutively express β-gal under the regulation of LacZ gene. Thus, cell differentiation and incorporation into the neovasculature of ischemic myocardium four weeks after surgery can be detected as β–gal$^+$ cells by immunohistochemistry. Double fluorescent immunostaining of ischemic myocardium 28 days after surgery revealed that β-gal-expressing EPCs (green) were frequently observed in ischemic border zone and co-localized with vessels perfused with BS-1 lectin (red) in the CD34$^+$ cell-injected group (Figure 6a). In contrast, a few KSL, KL and SL cells were observed in the ischemic border zone and incorporated into vessels (Figure 6a). Quantitative analysis for cell retention demonstrated that the number of

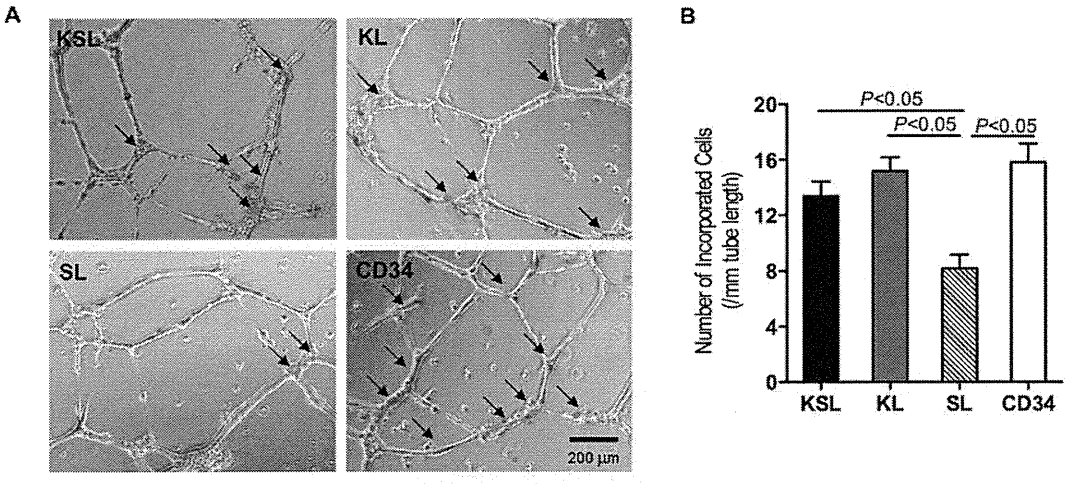

Figure 4. Tube formation assay by HUVECs incorporated with KSL, KL, SL, and CD34$^+$ cells. KSL, KL, SL, and CD34$^+$ cells were isolated via FACS and stained with DiI. DiI-labeled cells and HUVECs were seeded onto Matrigel-coated 96 well plates in 1% FBS/EBM2-MV without growth factors. After 24 hours in culture, incorporation of each cell population into tube-like structures formed with HUVECs was evaluated under fluorescence microscopy. a, Incorporated DiI positive cells were indicated by arrows. b, Number of incorporated DiI positive cells into tube-like structures was counted and averaged. All assays were triplicated and demonstrated similar results.
doi:10.1371/journal.pone.0020219.g004

incorporated cells into neovasculature was significantly higher in the CD34$^+$ cell-injected group than those in the other groups (Figure 6c).

In order to evaluate the size of MI, Masson's trichrome staining was performed with heart sections at day 28. Representative images indicated that fibrosis area was stained in blue and intact

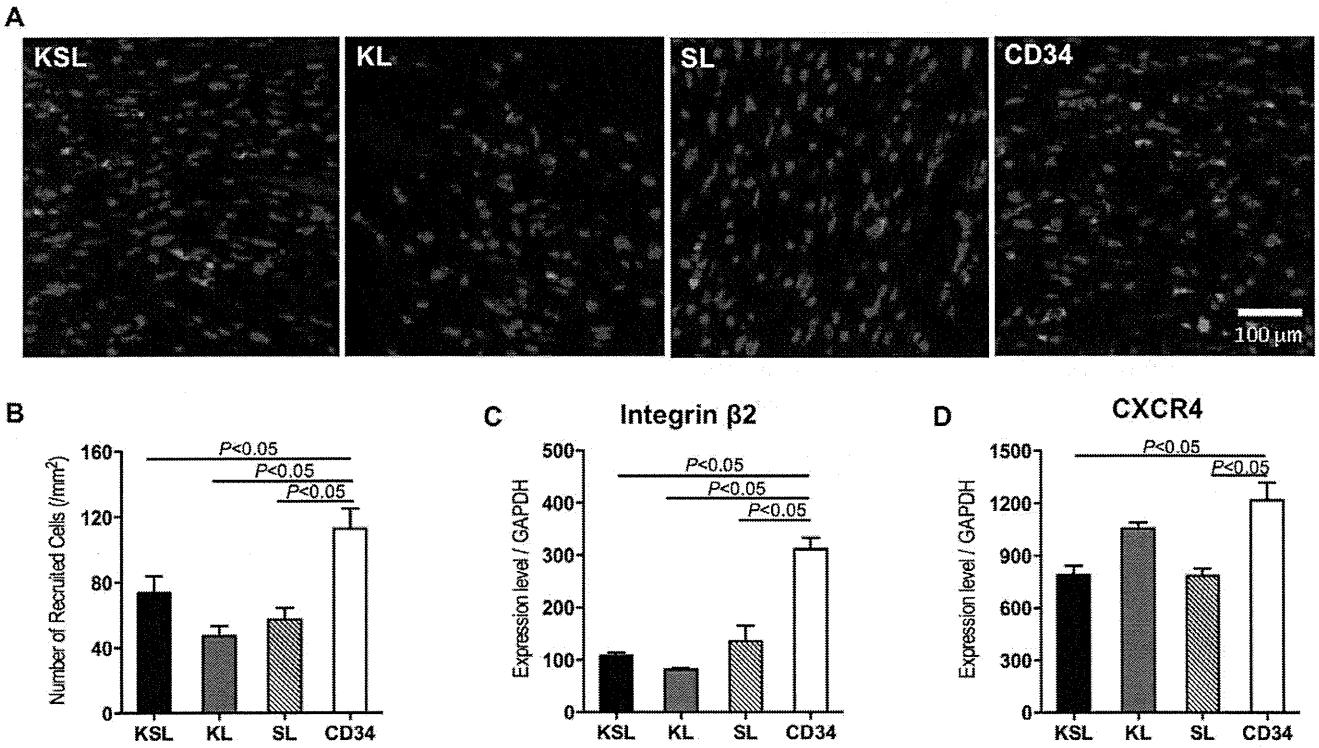

Figure 5. Assessment of cell recruitment and detection of homing molecules in KSL, KL, SL, and CD34$^+$ cells. KSL, KL, SL, and CD34$^+$ cells were freshly isolated by FACS and stained with DiI. DiI-labeled cells were systemically injected into mice three days after MI induction, and heart samples were examined histologically one day after cell injection. a, DiI positive cells (red) detected in ischemic myocardium under a fluorescence microscope. b, Number of DiI positive cells was counted in the ischemic border zone (bilateral sides of peri-infarct area) and averaged (n = 3). c and d, KSL, KL, SL, and CD34$^+$ cells were freshly isolated by FACS, and Integrin β2 and CXCR4 gene expression levels of these cells were examined by quantitative real-time RT-PCR. All assays were triplicated and demonstrated similar results.
doi:10.1371/journal.pone.0020219.g005

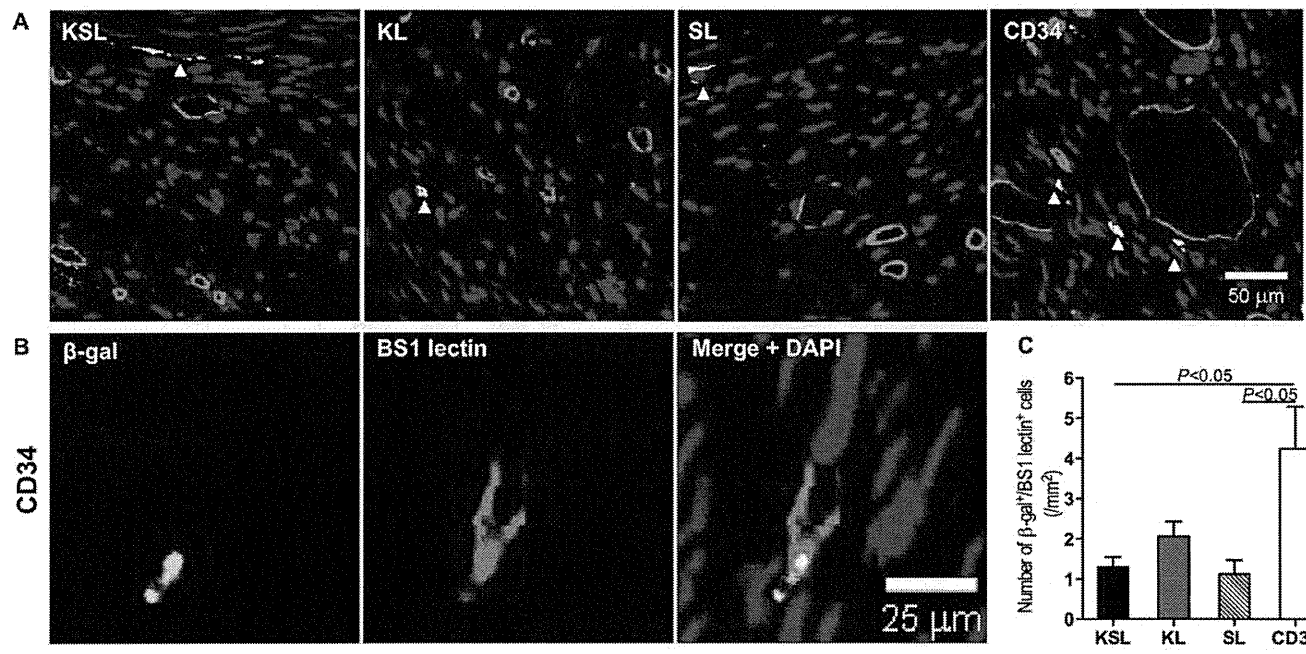

Figure 6. Assessment of cell incorporation into the neovasculature of the ischemic myocardium. KSL, KL, SL, and CD34$^+$ cells were isolated by FACS from GtRosa26 transgenic mice expressing LacZ gene universally, and were systemically injected three days after MI induction. Heart samples were harvested following BS1 lectin systemic perfusion 28 days after cell injection. a, Recruited cells visualized by immunofluorescent staining for β-gal (green) and BS1 lectin perfused capillaries (red) were shown in all groups. Recruited cells co-localizing with capillaries were marked by arrowheads and shown in yellow. b, A representative confocal image from the CD34$^+$ cell-injected group. c, The numbers of recruited cells that co-localized with capillaries were counted under a fluorescence microscope separately and averaged.
doi:10.1371/journal.pone.0020219.g006

myocardium was stained in red (Figure 7a). Quantitative analysis revealed that both the percent of fibrosis area in entire LV cross-sectional area and the percent of scar length in entire internal LV circumference were significantly reduced in the CD34$^+$ cell-injected group compared with the KSL cell-injected group, the SL cell-injected group and PBS group (Figure 7b and 7c). The staining of in vivo-perfused BS1 lectin and α-smooth muscle actin reflects angiogenesis in functional vessels in the peri-infarct myocardium four weeks after MI in all groups (Figure 8a and 9a). The averaged capillary density in the bilateral ischemic border zones of LV, an index of neovascularization, was significantly greater in the CD34$^+$ cell-injected group compared to the KSL cell-inject group and PBS group (CD34: 165±40/mm^2, KL: 150±25/mm^2, SL: 103±35/mm^2, KSL: 80±21/mm^2, PBS: 70±13/mm^2; $P<0.05$, PBS vs CD34 and KL, KSL vs CD34 and KL) (Figure 8b). Although the averaged number of arterioles was higher in the CD34$^+$ cell-injected group, no significant difference could be found between any two groups (Figure 9b). The KL cell-injected group also showed an increase in capillary density ($P<0.05$, KL vs KSL and PBS), reduced fibrosis area ($P<0.05$, KL vs KSL and PBS) and reduced fibrosis length ($P<0.05$, KL vs KSL, SL and PBS).

Transplanted CD34$^+$ cells effectively preserve LV function after MI

There were no significant differences in preoperative echocardiographic parameters, LVEDD (left ventricular end-diastolic dimension), LVESD (left ventricular end-systolic dimension), EF (ejection fraction) and FS (fractional shortening) among any groups. Echocardiography performed 7 days and 28 days after cell transplantation demonstrated that ΔLVEDD (day 28-day 7) was significantly smaller in the CD34$^+$ cell-treated group than in the PBS-, the KSL- and the SL-treated groups ($P<0.05$ vs PBS, KSL and SL) (Figure 10a). The ΔLVEDD was also significantly smaller in the KL-treated group than in the PBS- and the KSL-treated groups ($P<0.05$) (Figure 10a). However, ΔLVEDD was similar in the PBS-, the KSL- and the SL-treated groups (Figure 10a). The ΔLVESD (day 28-day 7) was significantly smaller in the CD34$^+$ cell-treated group than in the PBS-, the KSL- and the SL-treated groups ($P<0.05$ vs PBS, KSL and SL) (Figure 10b). The ΔEF (day 28-day 7) was significantly greater in the CD34$^+$ cell-treated group than in the PBS-, the KSL- and the SL-treated groups ($P<0.05$ vs PBS, KSL and SL) (Figure 10c). The ΔEF was also significantly smaller in the PBS-treated group than in the KSL-, the KL- and the SL-treated groups ($P<0.05$) (Figure 10c). The ΔFS (day 28-day 7) was significantly greater in the CD34$^+$ cell-treated group than in the PBS-, the KSL-, the KL- and the SL-treated groups ($P<0.05$ vs PBS, KSL, KL and SL) (Figure 10d). The ΔFS was also significantly smaller in the PBS-treated group than in the KSL-, the KL- and the SL-treated groups ($P<0.05$) (Figure 10d). Overall, transplantation of CD34$^+$ cells exhibited significant LV functional recovery among all cell-transplanted groups following MI, which is consistent with the results of histological analysis.

Discussion

The present study was designed to determine a functional population for murine EPC transplantation by systemic injection. The results indicated the CD34 could be a better marker for isolating functional EPC populations in mouse bone marrow compared with c-Kit, Sca-1 and their combination. We have demonstrated that mouse bone marrow-derived CD34$^+$ cells exhibit characteristics of endothelial progenitors both in vitro and in vivo as follows: 1) CD34$^+$ cells possess highly adhesive feature

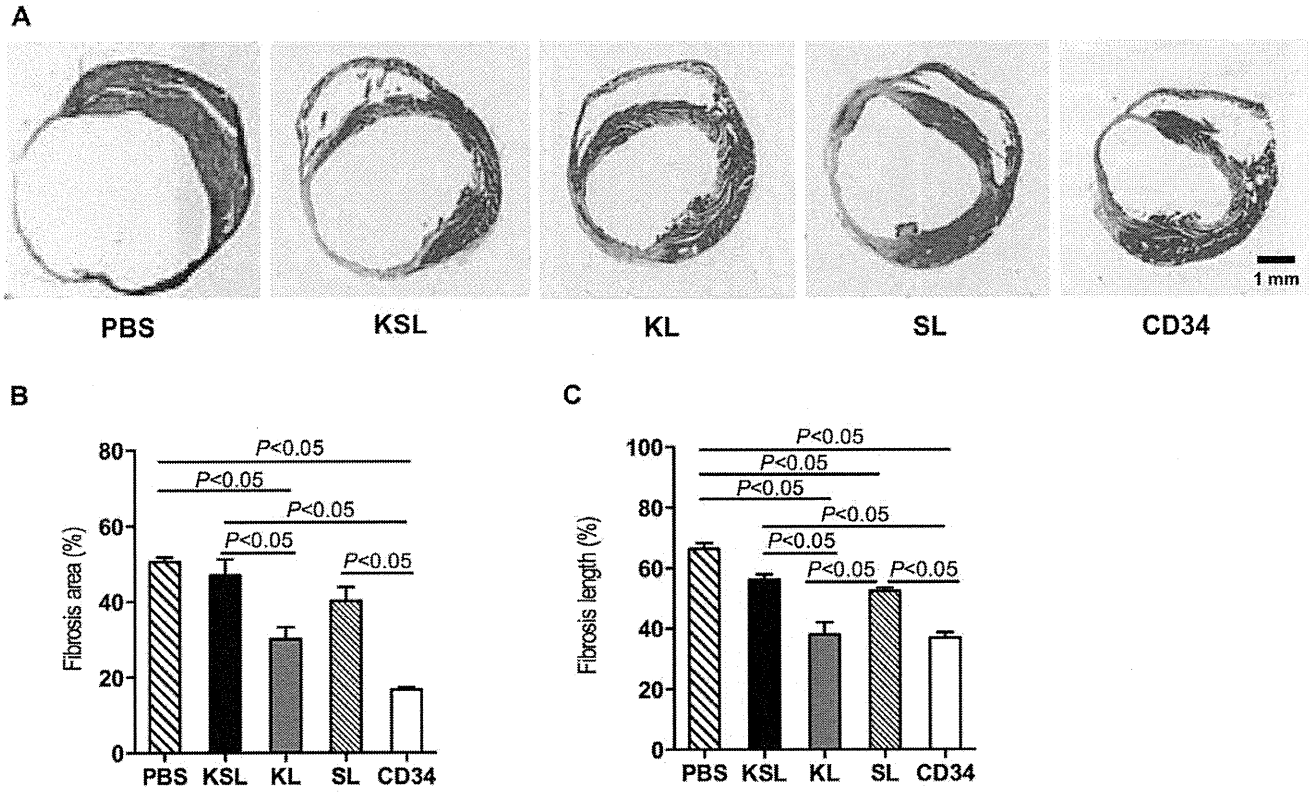

Figure 7. Histological analysis for MI size in ischemic myocardium. KSL, KL, SL, CD34$^+$ cells and PBS control were systemically injected 3 days after MI induction. Heart samples were harvested following BS1 lectin systemic perfusion 28 days after cell injection. a, Heart sections were stained by Masson's Trichrome staining. Red indicates intact myocardium and blue indicates scared fibrosis area. b, The percent of fibrosis area in entire LV cross sectional area was calculated and averaged (n = 3). c, The percent of scar length in internal LV circumference was calculated and averaged (n = 3).
doi:10.1371/journal.pone.0020219.g007

and highly express endothelial markers following the conversion to an adhesive cell phenotype despite of their less colony forming capacity, 2) CD34$^+$ cells have a better homing capacity to ischemic tissue through adhesion molecule and chemokine/receptor-dependent mechanism, and 3) Recruited CD34$^+$ cells are frequently incorporated into functional vessels contributing to the reduction of MI size, the enhanced angiogenesis and the significant LV functional recovery following MI.

Since phenotypic HSCs (c-Kit$^+$/Sca-1$^+$/Lin$^-$ cells) [29] have been described to have the ability to give rise to endothelial progeny [30,31,32], KSL cells have been widely used as mouse EPCs [13,14,15,16], displaying colony forming capacity, endothelial differentiation capacity and vasculogenic activity. In addition, Takahashi et al [2] used Sca-1$^+$ cells from peripheral blood as an EPC-enriched population and demonstrated their differentiation into endothelial cells in mice with hindlimb ischemia. Cheng et al [17] purified CD31$^+$/c-Kit$^+$/Lin$^-$ cells from bone marrow and confirmed their contribution to neovascularization following bone marrow transplantation. Very recently, Kim et al [33] has demonstrated high vasculogenic property of CD31 positive cells in BMMNCs. On the other hand, Balsam et al [34] and Murry et al [35] reported that mouse bone marrow HSCs isolated as c-Kit$^+$/Lin$^-$ cells or c-Kit$^+$/Sca-1$^+$/Thy1.1^{lo}/Lin$^-$ cells adopt mature haematopoietic fates in the infarcted myocardium. Given the controversy and also considering that CD34 expression patterns during early mouse development are related to modes of blood vessel formation [7], we analyzed the EPC properties of mouse bone marrow derived c-Kit$^+$/Sca-1$^+$/Lin$^-$ cells (KSL), c-kit$^+$/Lin$^-$ cells (KL), Sca-1$^+$/Lin$^-$ cells (SL) and together with CD34$^+$ cells. As for the adherent EPC formation, CD34$^+$ cells and KL cells changed their phenotypes more frequently into adherent cells than the others. We also examined mRNA and protein expressions in CD34$^+$, KSL, KL and SL cells cultured under an endothelial culture condition. Although immunocytochemistry revealed that VE-cadherin, vWF and Flk-1 were similarly positive in all types of cells, mRNA expression of these markers was greatest in CD34$^+$ cells, suggesting that endothelial differentiation may occur more robustly in CD34$^+$ cells than in the others. We also examined the expressions of CD45 and another EC marker CD146. CD45 and CD146 were expressed partially in the cells in each group (Figure S3), suggesting that the cells were partially differentiated exhibiting both hematopoietic and endothelial phenotypes. A few cells also expressed CD34 during the culture (Figure S3).

The cell homing capacity to ischemic tissue is also one of the unique characteristics in EPCs. The major distinct assortment of EPCs is proposed to lay in their *in vivo* phenotype, distinguishing "circulating EPCs" from "tissue EPCs". Circulating EPCs can be isolated from PB and BM and represent a population of suspended non-adhesive cell phenotype. These cells migrate from their initial protective niches in the BM into the blood stream, and home via the circulatory system to sites undergoing vascular regeneration and repair, transforming into local adhesive tissue EPCs. Therefore, we further examined EPC groups regarding the biological properties for homing *in vitro* and the pathophysiological recruitment from circulation *in vivo* using a mouse MI model. The most dramatic cell recruitment to ischemic myocardium immediately after MI was observed in the CD34$^+$ cell-injected group.

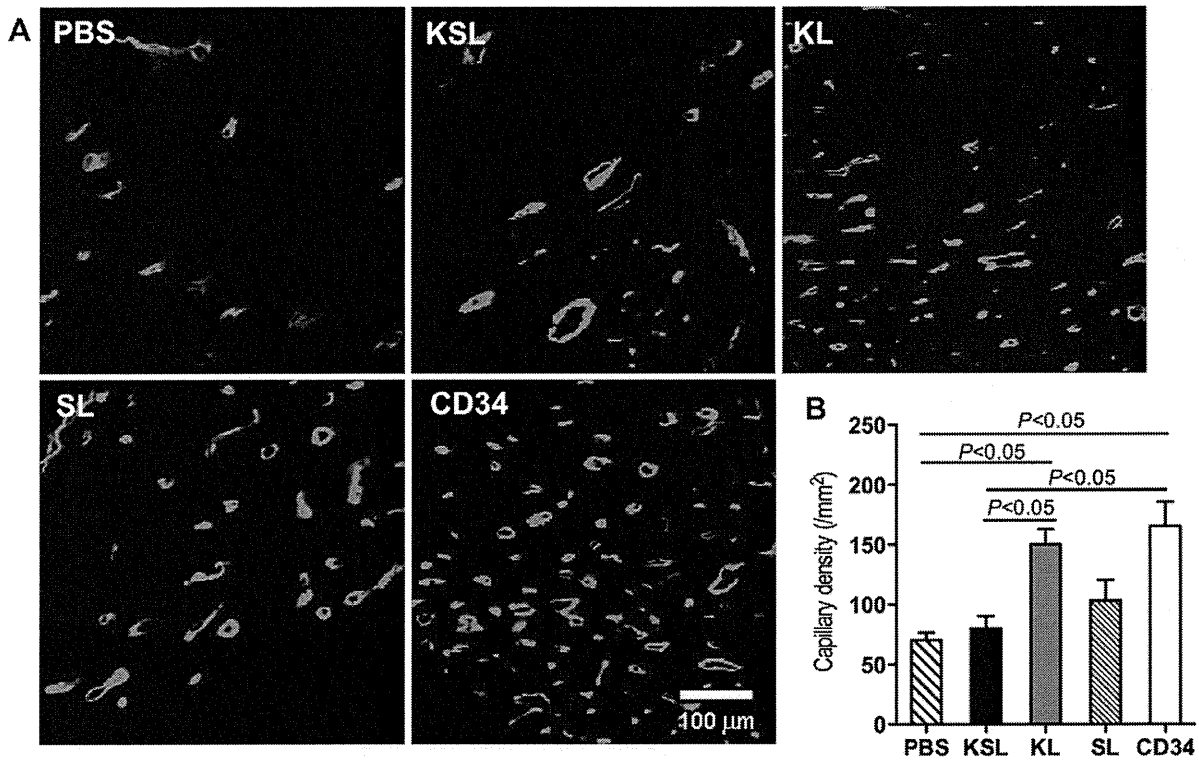

Figure 8. Histological analysis for capillary density in ischemic myocardium. KSL, KL, SL, CD34+ cells and PBS control were systemically injected 3 days after MI induction. Heart samples were harvested following BS1 lectin systemic perfusion 28 days after cell injection. a, Capillaries were visualized as tubular structure perfused by BS1 lectin. b, The numbers of capillaries were counted in bilateral sides of the peri-infarct zone on LV cross sections and averaged in each group (n = 3), respectively.
doi:10.1371/journal.pone.0020219.g008

Integrinβ2 and CXCR4 have been reported previously to be critical for the homing and neovascularization capacity of EPCs. They were significantly up-regulated in CD34+ cells compared to the others by RT-PCR analysis, providing a very possible explanation for the most striking cell recruitment of CD34+ cells to ischemic myocardium. In fact, we also assessed many angiogenic factors including VEGFs, Ang-1, IGF, PLGF and SCF in all types of cells, but the expression levels of all these genes were similar among them (data not shown). Therefore, the homing activity is one of the crucial mechanisms in regard to revascularization. With the most homing and recruited cells, the CD34+ cell-injected group performs the best. It is noteworthy that CD34+ cells and KL cells showed a similar adhesive capacity in vitro, while in vivo they didn't. We speculate that it is caused by the up-regulated expressions of integrinβ2 and CXCR4 in CD34+ cells. Furthermore, the highest number of cells was incorporated into vascular structure in the CD34+ cell-injected group in the 28 days follow up study, resulting in the reduced fibrosis, the increased vascularity and the significantly enhanced LV functional recovery in the ischemic myocardium. Another finding is that KL cell-injected group also showed greater capillary density and smaller fibrosis area/length than SL and KSL groups, possibly due to more abundant incorporation into neovasculature. Since myocardial regeneration requires vascular regeneration and cardiomyocyte regeneration as well, the recruited cells might differentiate into cardiomyocytes in addition to endothelial cells, as we observed for human CD34+ cells [36].

To make sure that vasculogenesis and the observed recruitment capacities of mouse bone marrow CD34+ cells indeed reflect the characteristics of EPCs rather than mature endothelial cells (ECs), we analyzed the presence and expression of several other cell surface markers such as CD31, VE-cadherin, Flk-1 and Tie-2 in the CD34+ cell population by FACS analysis (Figure S4). Positive percentages of CD31, VE-cadherin, Flk-1 and Tie-2 were 83%, 0.5%, 1.1% and 4%, respectively, indicating that no substantial EC contamination of CD34+ cells is present.

In the conventional EPC culture, two major cell types have been shown to emerge out of MNC cultures: EC-like cells (i.e., early EPC, cultured EPC) and endothelial outgrowth cells (i.e., EOCs) [37]. While EOCs are proved to derive from endothelial colony forming cells (ECFCs), EC-like cells have not been identified to develop from any colony forming unit, although CFU-EC was initially presumed as an origin of EC-like cells, but was later defined as an aggregate of hematopoietic cells and EPCs. Lately, a new EPC colony forming assay (EPC-CFA) has been developed, challenging some of the classical views predominant in the field and opening the possibility to illustrate the developmental hierarchy of EPCs [15,16,22,38]. The methodological concept of EPC-CFA was recently introduced and further developed for the use of human EPCs (Masuda et al., revising in Circulation Research). In this research, small-EPCs are characterized as "primitive EPCs", which are possibly derived from further immature and proliferative EPCs, and large-EPCs as "definitive EPCs" which are more prone to differentiation and promoting EPC-mediated cell functions required for vasculogenesis. The definitive EPCs are capable of differentiating into a non-colonizing large EPC phenotype, similar to "EC-like cells (i.e., early EPC, cultured EPC)" detected by conventional EPC culture [39,40,41]. Therefore, "EC-like cells" are speculated to represent further differentiating EPCs, departed from the niche of colony forming

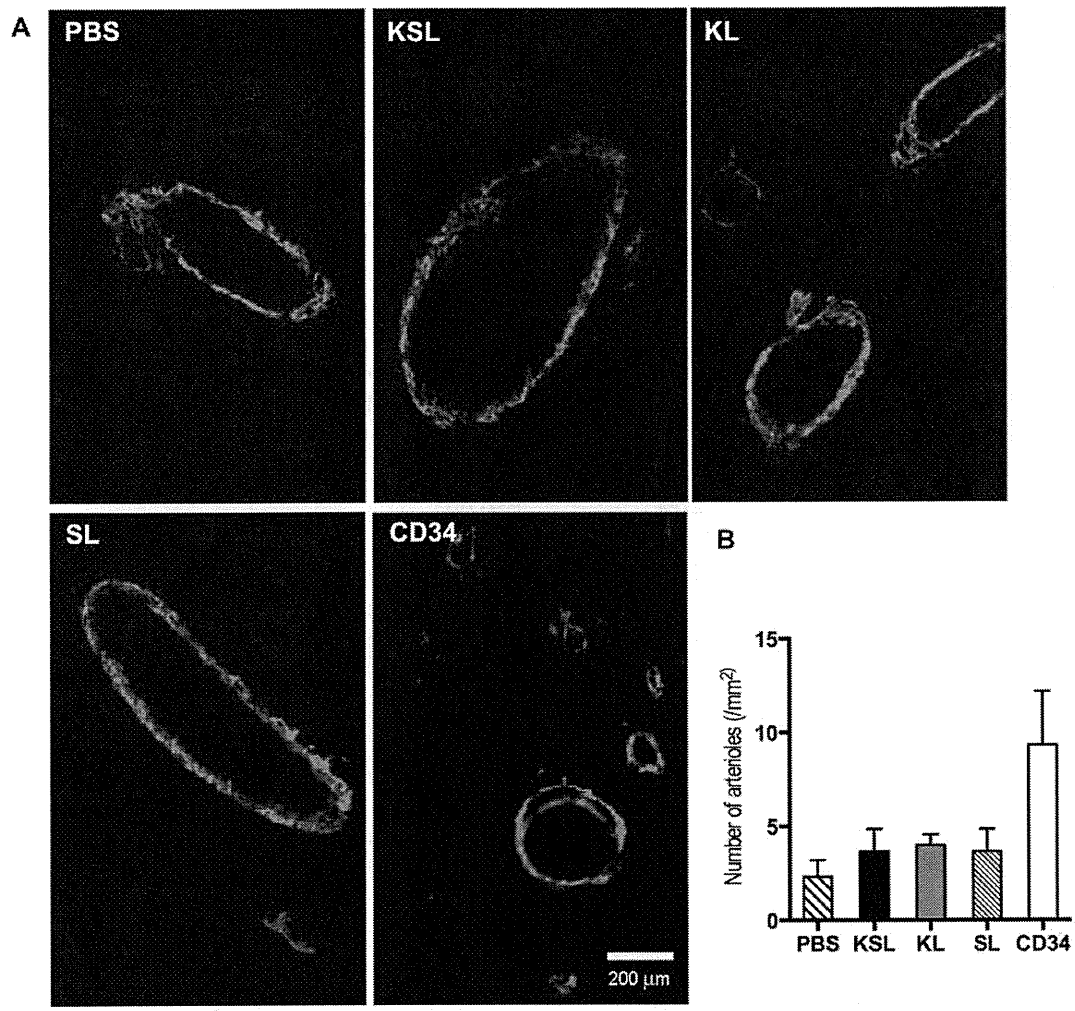

Figure 9. Histological analysis for arterioles in ischemic myocardium. KSL, KL, SL, CD34$^+$ cells and PBS control were systemically injected 3 days after MI induction. Heart samples were harvested following BS1 lectin systemic perfusion 28 days after cell injection. a, Arterioles were visualized following α-smooth muscle actin staining. b, The numbers of arterioles were counted in bilateral sides of the peri-infarct zone on LV cross sections and averaged in each group (n = 3), respectively.
doi:10.1371/journal.pone.0020219.g009

EPCs such as small- and large-EPCs. In contrast, EOCs demonstrate very similar expressional profiles and biological functions to differentiated ECs such as human umbilical vein ECs and human microvascular ECs, and are considered to be generated from different stem cell fraction compared to EC-like cells as previously reported [42,43,44]. Later studies by Case et al or Timmermans et al demonstrated that CD34$^+$CD133$^+$VEGFR-2$^+$ or CD133$^+$ cells are hematopoietic progenitor cells that do not yield EOCs [44,45]. These findings support the idea that EOCs are not likely to derive from hematopoietic stem cells (HSCs) or hematopoietic progenitor cells (HPCs) originating from the BM, while EC-like cells and two types of colonies in EPC-CFA are relating to HSCs or HPCs. Therefore, the primary and original phenotype of EPC-CFA and EC-like cells seems different from EOCs (ECFCs), though it is not conclusive due to the immaturity in respective EPC biology.

In terms of EPC colony forming activity, KSL cells formed a substantially greater number of small (primitive) EPC colonies and large (definitive) EPC colonies, especially small EPC colony forming activity of KSL cells was robust compared to the others, which is consistent with our previous data [16]. Both KL cells and SL cells showed a less level of small/large colony forming activity, while CD34$^+$ cells demonstrated a further low activity. In the cell culture assay and in vivo assays, CD34$^+$ cells had the highest activity. It seems to be controversial that CD34$^+$ cells are the most functional cells, but they can only form a few colonies. In fact, it is not surprising and very reasonable. Because CD34$^+$ cells count 12.23±0.02% in BMMNCs, while KL cells count 3.737±0.004%, SL cells count 1.327±0.001%, KSL count 0.597±0.001%, respectively, which indicates CD34$^+$ cells are partially differentiated cells. In EPC differentiation hierarchy, it was confirmed that small EPC colonies are capable of differentiation into large EPC colonies and that large colonies can further differentiate into adherent, more vasculogenic EPCs in culture (unpublished data by Masuda et al) (Figure 11). In addition, small EPC colonies have a predominant stem cell-like potential for proliferation and large EPC colonies possess a predominantly vasculogenic potential including cell adhesion, tube formation activity in vitro and contribution to de novo blood vessel formation in ischemic tissue (Kwon et al [16], unpublished data by Masuda et al and Tsukada et al and Figure S2) (Figure 11). Taken the EPC differentiation and in vivo data together, our results suggest that KSL cells are most

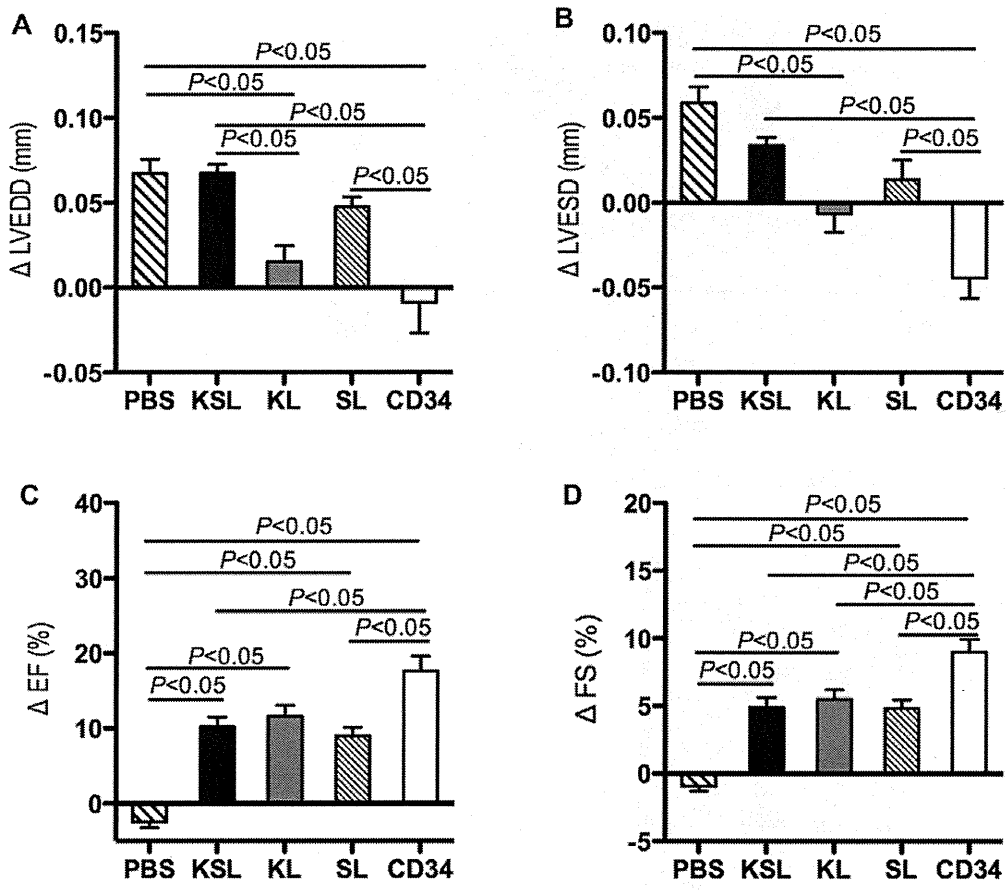

Figure 10. Functional analysis of treated hearts by echocardiography. Echocardiographic parameters for cardiac function 28 days vs. 7 days after myocardial infarction and treatments. The following parameters: left ventricular end diastolic diameter (LVEDD) (a), left ventricular end systolic diameter (LVESD) (b), left ventricular ejection fraction (EF) (c) and left ventricular fractional shortening (FS) (d) were measured in the PBS-, the KSL-, the KL-, the SL- and the CD34$^+$ cell-injected groups, and change of each parameter between day 7 and day 28 after surgery was calculated and averaged (n = 3).
doi:10.1371/journal.pone.0020219.g010

immature, while CD34$^+$ cells are most differentiating population in mouse EPCs that we studied (Figure 11). Therefore we hypothesize the possible differentiation hierarchy of KSL, KL, SL and CD34$^+$ cells (Figure 11).

Consequently, our data demonstrates that CD34 may be a better and more suitable marker for mouse functional EPCs with higher homing and vasculogenic properties, which could benefit the investigation of therapeutic EPC biology. Assuming the heterogeneity of CD34$^+$ population, more vasculogenic fraction co-expressing another marker may exist in the mouse bone marrow CD34$^+$ cells. The search for a truly selective EPC marker, marking "real" EPCs in combination with CD34, has thus to be continued.

Materials and Methods

Animals

C57BL6/J mice (male, 8–12 weeks old) were used for all experiments. Transgenic mice that constitutively expressβ-galactosidase (β-gal) under the control of the LacZ gene (B6;129S-Gt[ROSA]26Sor/J, male, 8–12 weeks old) were purchased from Jackson Laboratories (ME, USA) and used for in vivo experiments in which genetically labeled (positive for the LacZ gene) 50,000 SL, KL, KSL and CD34$^+$ cells were systemically injected into wild type recipient mice after MI surgery.

Preparation of KSL, KL, SL and CD34$^+$ Cells

Bone marrow cells were harvested from hipbones, femurs, tibiae, shoulder bones, ulnas, vertebra and sternum of mice. BMMNCs were isolated from total bone marrow cells by subsequent purification over Histopaque gradients. BMMNCs of WT and ROSA26 mice were incubated with FITC-conjugated anti-CD34 antibody (BD Pharmingen) for 30 minutes at 4°C and CD34$^+$ cells were further isolated using FACS Aria (BD Biosciences). For SL, KL and KSL cell isolation, BMMNCs were incubated with a cocktail of biotinylated monoclonal antibodies against lineage markers (BD IMag) for 15 minutes at 4°C. These cells were further incubated with streptavidin-conjugated magnetic nanoparticles (BD IMag) for 30 minutes. After depletion of lineage positive cells, lineage negative cells were subsequently incubated with PE-conjugated anti-Sca-1 antibody, (BD Pharmingen), APC-conjugated anti-c-Kit antibody (BD Pharmingen) and APC Cy7-conjugated streptavidin (BD Pharmingen) for 30 minutes at 4°C followed by isolation of the desired different sub-fractions KSL, KL and SL by FACS Aria (BD Biosciences).

EPC Colony Forming Assay

The number of EPC colonies was assessed by EPC colony forming assay that we have developed recently [16,22]. The KSL, KL, SL and CD34$^+$ cells (500 cells/well) were cultured in methyl

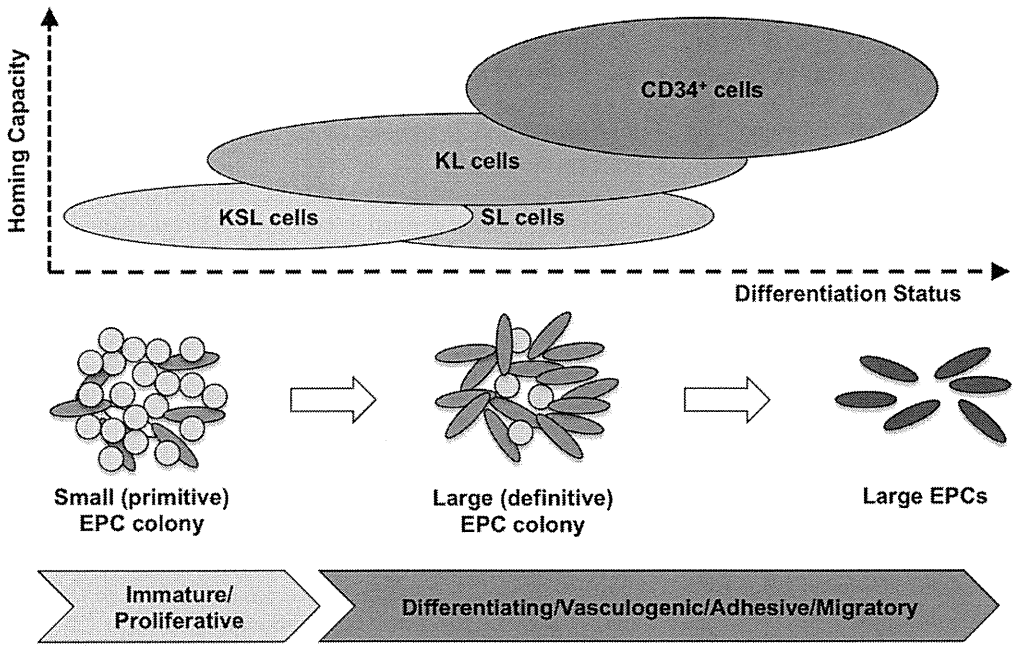

Figure 11. Stem/progenitor differentiation hierarchy of KSL, KL, SL and CD34$^+$ cells. In EPC-CFA, small EPC colonies are capable of differentiating into large colonies and large EPC colonies can further differentiate into adherent, more vasculogenic non-colony forming EPCs in culture. Small colonies reveal a predominant potential for proliferation, while large colonies demonstrate a predominantly vasculogenic potential including cell adhesion and tube-like structure formation in vitro (unpublished data, lower panel). Based on the EPC colony numbers of KSL, KL, SL and CD34$^+$ cells, the conceivable extent of homing capacity (Y-axis) and differentiation status (X-axis) in each cell type is indicated in the upper panel.
doi:10.1371/journal.pone.0020219.g011

cellulose-containing medium M3236 (StemCell Technologies, Vancouver, Canada) with the following supplements in 6-well culture plates (Primaria, BD Falcon) for 7 days: 50 ng/ml of vascular endothelial growth factor (VEGF) (R&D Systems, MN), 20 ng/ml of stem cell factor (SCF) (KIRIN, Japan), 50 ng/ml of epidermal growth factor (EGF) (Wako, Japan), 20 ng/ml of interleukin-3 (KIRIN, Japan), 50 ng/ml of insulin-like growth factor-1 (IGF-1) (Wako, Japan), 50 ng/ml of basic fibroblast growth factor (bFGF) (Wako, Japan), 2 U/mL of heparin (AJINOMOTO, Japan) and 10% FBS. EPC-Colony Forming Units (CFUs) were identified as large-EPC-CFUs or small-EPC-CFUs by visual inspection with an inverted microscope under 40× magnification. Large-EPC-CFUs are mainly composed of spindle-shaped cells whereas small-EPC-CFUs are aggregates of small round cells. The endothelial phenotype of the EPC colonies was confirmed by their high up-take of acetylated low density lipoprotein (acLDL, Biomedical Technologies Inc, Stoughton, MA) and immunocytochemical positivity for isolectin B4 (Molecular Probes, CA). The total numbers of colonies with small-EPC-CFUs and large-EPC-CFUs were counted in the entire view fields of each culture plate and averaged.

Collection and phenotypes of small and large colonies

After removal of methylcellulose containing floating and hematopoietic cells by cold PBS (1 ml/well) in 6-well plates, white spotty colonies (small colonies) were flushed gently with 1 ml of cold PBS for 3 times and collected. One ml of cold EDTA/PBS (5mmol/L) was then added to each well. The plates were then incubated for 5 minutes at 37°C and large colonies were collected. Small colonies and large colonies were incubated with PE-conjugated anti-CD19 antibody, PE-conjugated anti-CD3 antibody, PE-conjugated anti-CD14 antibody, PE-conjugated anti-CD41 antibody, PE-conjugated anti-CD31 antibody, PE-conjugated anti-Flk-1 antibody, PE-conjugated anti-Tie-2 antibody, PE-conjugated anti-Sca-1 antibody, APC-conjugated anti-VE-cadherin antibody, APC-conjugated anti-CD45 antibody, APC-conjugated anti-c-Kit antibody (BD Pharmingen), respectively, for 30 minutes at 4°C.After washing with PBS for 2 times, cells were analyzed by FACS Aria (BD Biosciences).

EPC Culture Assay

Cellular adhesion capacity was evaluated as described previously [46]. Briefly, freshly isolated cells (10^5 cells/well) were seeded in 20% fetal bovine serum (FBS)/EGM-2MV medium (Lonza) on a 8-well chamber slide coated with ProNectin F (Sigma), and cultured for 7 days at 37°C under 5%CO_2. Each well was then washed 3 times with PBS and the attached cells were fixed with 4% paraformaldehyde (PFA)/phosphate buffer saline (PBS) and stained with DAPI. The attached cells were visualized under a fluorescence microscope and counted. The adhesive activity of each cell group was evaluated as the mean number of attached cells in each group.

Immunocytochemistry

Cell samples were prepared for EPC culture assay as described above. Each cell-containing well was then washed three times with PBS and attached cells were briefly fixed with 4% PFA/PBS. For improved detection of intracellular proteins, cells were permeabilized by incubation in 0.1% Triton X-100/PBS solution for 5 min at room temperature (RT) followed by a three time rinse with PBS. Samples were blocked in antibody dilution buffer 2% BSA/PBS for 1 hour at RT. After removal of the blocking solution, primary antibodies were added: anti-VE-cadherin antibody (Santa Cruz, 1:100), anti-vWF antibody (Chemicon, 1:100), anti-Flk-1 antibody (Chemicon, 1:100), anti-CD45 antibody (Abcam, 1:200), anti-CD34 antibody (Abcam, 1:50), anti-CD146 antibody (Abcam,

1:100) in antibody dilution buffer at 4°C overnight. After washing three times with PBS for 5 min each, cells were incubated with secondary antibodies prepared at 1:500 in antibody dilution buffer: Alexa 488 donkey anti-goat IgG, Alexa 488 goat anti-rabbit IgG and Alexa 488 goat anti-rat IgG (MP/Invitrogen) for 30 min at RT. After secondary antibodies were removed and cells were washed with PBS for three times, DAPI solution (Sigma, 1:5000) was added and nuclei were stained for 10 min at RT. Mounting medium and a cover-slip were added to the glass slide followed by sealing samples with nail varnish before evaluation of the staining results under fluorescence microscopy.

Quantitative Real-time RT-PCR

Total RNA was isolated from cell samples using RNeasy Mini kit (QIAGEN) according to the manufacturer's instructions. cDNA was synthesized using PrimeScript RT reagent Kit (TAKARA BIO Inc., Japan). For quantitative RT-PCR, the converted cDNA samples (2 μl) were amplified in triplicate in a final volume of 10 μl using SYBR Green Master Mix reagent (Applied Biosystems) and gene-specific primers with an ABI Prism 7700 RT-PCR machine (Applied Biosystems). Melting curve analysis was performed with Dissociation Curves software (Applied Biosystems) and the mean cycle threshold (Ct) values were used to calculate gene expression levels with normalization to mouse GAPDH.

RT-PCR Primers

mGAPDH: forward: ACATCATCCCTGCATCCACT; reverse: CACATTGGGGGTAGGAACAC, mvWF: forward: ACGCCATCTCCAGATTCAAG, reverse: AAGCATCTCCCACAGCATTC, mVE-Cadherin: forward: TACTCAGCCCTGCTCTGGTT, reverse: GCTTGCAGAGGCTGTGTCTT, mFlk-1: forward: GGGTTTGGTTTTGGAAGGTT, reverse: CACGTAAGAGTCCGGAAGGA, mIntegrin beta 2: forward: GTACAGGCGCTTTGAGAAGG, reverse: TTTCAGCAAACTTGGGGTTC, mCXCR4: forward: TGCTGTGTGATGGTTTGTTTG, reverse: AAACCCCCAGCATTTCTACC.

In Vitro Incorporation Assay

HUVECs and freshly isolated cells were used for tube formation assays as described previously [46]. CD34$^+$, SL, KL, and KSL cells were labeled with DiI for 20 minutes. After washing with PBS, 2,000 of the DiI-labeled cells were mixed with 40,000 HUVECs in 100 μL of 10% FBS/EGM-2MV medium (Lonza) in order to evaluate the contribution of EPCs to EC-derived tube formation. One hundred μl of cell suspensions were applied to 100 μl of Matrigel (BD Biosciences) coated wells in an 8-well glass chamber slide (BD Falcon), and then incubated for 48 hours. The number of formed tubes and incorporated DiI-labeled cells were counted and averaged with the help of a computer assisted fluorescent microscope (OLYMPUS, Japan).

Surgical Procedure

Institutional Animal Care and Use Committee in Institute of Biomedical Research and Innovation and RIKEN Center for Developmental Biology approved all the following research protocols (approval ID: AH21-01), including surgical procedures and animal care. Mice were anesthetized with 0.015 mg/kg of Avertin^{TM} (Sigma). Myocardial infarction (MI) was induced as described previously [47]. Briefly, after the fourth to fifth intercostal space was opened, the heart was exteriorized and the pericardium was incised. Thereafter, the heart was held with a fine forceps, and MI was induced by ligation of the left anterior descending coronary artery at the just proximal site of the bifurcation of a diagonal branch with a 7-0 nylon suture followed by thorax closure. For in vivo study, 50,000 KSL, KL, SL and CD34$^+$ cells together with PBS control were systemically injected 3 days after MI.

Physiological Assessment of LV Function Using Echocardiography

Transthoracic echocardiography (SONOS 5500, Philips Medical Systems) was performed to evaluate LV function immediately before and 7 and 28 days after MI. After anesthesia with Avertin^{TM} (Sigma), left ventricular end diastolic diameter (LVEDD), left ventricular end systolic diameter (LVESD), left ventricular ejection fraction (EF) and left ventricular fractional shortening (FS) were measured at the midpapillary muscle level. All procedures and analysis were performed by an experienced researcher who was blinded to treatment.

Tissue Harvesting

For cell recruitment studies, MI-induced mouse hearts were harvested 24 hours after cell injection and prepared for frozen tissue sectioning after fixation with 4% PFA/PBS. For cell retention studies, MI-induced mice were anesthetized 28 days after surgery. Griffonia (Bandeiraea) Simplicifolia lectin 1 (Vector, 0.1 mg per mouse) was then injected systemically by direct cardiac puncture. Ten minutes later, the animals were euthanized, and hearts were harvested and prepared for paraffin tissue sectioning after fixation with 4% PFA/PBS.

Morphometric Evaluation of Infarct Size

To elucidate the severity of myocardial fibrosis, Masson trichrome staining was performed on frozen sections from each tissue block, and the stained sections were used to measure the average ratio of fibrosis area to entire LV cross-sectional area (percent fibrosis area) and the average ratio of fibrosis length to entire internal LV circumference (percent fibrosis length).

Immunofluorescence Staining

The sections were stained with rabbit anti-β-gal antibody (Cortex, 1:1000) and antibody to Griffonia (Bandeiraea) Simplicifolia lectin 1 (Vector, 1:100), then washed with PBS and stained with Alexa Fluor 488 rat anti-rabbit IgG and Alexa Fluor 546 rabbit anti-goat IgG (MP/Invitrogen, 1:1000) at RT for one hour. Nuclei were counterstained with DAPI (Sigma, 1:5000), and sections were mounted in aqueous mounting medium. Images were examined using a confoal microscope (OLYMPUS, Japan). To detect arterioles, the sections were stained with anti-α smooth muscle actin (SMA) antibody (Dako, 1:250), then washed with PBS and stained with Alexa Fluor 594 donkey anti-mouse IgG2a (MP/Invitrogen, 1:1000) at RT for one hour. Nuclei were counterstained with DAPI, and sections were mounted in aqueous mounting medium. Images were examined using a fluorescence microscope.

Statistical analysis

All values were presented as mean ± SEM. Statistical analyses were performed with commercially available software (GraphPad Prism^{TM}, MDF Co Ltd, Japan). Comparisons between multiple groups were tested for significance via analysis of variance (ANOVA) followed by post-hoc testing with the Tukey's procedure. A P value less than 0.05 was considered statistically significant.

Supporting Information

Figure S1 CD34 positivity in KSL, KL and SL cells. KSL cells were isolated from BMMNCs and further examined for

CD34 expression by FACS. The analyzed data was shown as histogram. The percent of CD34 positivity was indicated in each histogram.
(TIF)

Figure S2 Phenotypes of large and small colonies. Large colonies and small colonies were collected separately after 7 days culture in methylcellulose medium. Phenotypes of large colonies (a) and small colonies (b) were analyzed by FACS. The analyzed data was shown as histogram. The percent of each positive population was indicated in each histogram.
(TIF)

Figure S3 Assessment of CD45, CD146 and CD34 in cultured KSL, KL, SL, and CD34$^+$ cells by immunocytostaining. Freshly isolated cells were cultured in 20%FBS/EGM-2MV medium on vitronectin-coated 4 well-chamber slides for 7 days. Adherent cells were stained with CD45, CD146 and CD34. The assay was triplicated and demonstrated similar results.
(TIF)

Figure S4 Endothelial marker expressions in freshly isolated mouse CD34+ cells. CD34$^+$ cells were isolated from mouse BMMNCs (10^5 cells/mL) and further examined for CD31 (a), VE-cadherin (b), Flk-1 (c) and Tie-2 (d) expressions by FACS. The percent of each positive cell population was indicated in the contour plots.
(TIF)

Acknowledgments

The authors would like to thank the animal facility of *RIKEN Center for Developmental Biology* for providing the space to perform animal surgery.

Author Contributions

Conceived and designed the experiments: MI TA. Performed the experiments: JY MI. Analyzed the data: JY MI NK TA. Contributed reagents/materials/analysis tools: MI NK SK HA HM YS. Wrote the paper: JY MI CA AK TA.

References

1. Kawamoto A, Gwon HC, Iwaguro H, Yamaguchi JI, Uchida S, et al. (2001) Therapeutic potential of ex vivo expanded endothelial progenitor cells for myocardial ischemia. Circulation 103: 634–637.
2. Takahashi T, Kalka C, Masuda H, Chen D, Silver M, et al. (1999) Ischemia- and cytokine-induced mobilization of bone marrow-derived endothelial progenitor cells for neovascularization. Nat Med 5: 434–438.
3. Li Calzi S, Neu MB, Shaw LC, Kielczewski JL, Moldovan NI, et al. (2010) EPCs and pathological angiogenesis: when good cells go bad. Microvasc Res 79: 207–216.
4. Urbich C, Dimmeler S (2004) Endothelial progenitor cells: characterization and role in vascular biology. Circ Res 95: 343–353.
5. Andrews RG, Singer JW, Bernstein ID (1986) Monoclonal antibody 12-8 recognizes a 115-kd molecule present on both unipotent and multipotent hematopoietic colony-forming cells and their precursors. Blood 67: 842–845.
6. Baumheter S, Singer MS, Henzel W, Hemmerich S, Renz M, et al. (1993) Binding of L-selectin to the vascular sialomucin CD34. Science 262: 436–438.
7. Wood HB, May G, Healy L, Enver T, Morriss-Kay GM (1997) CD34 expression patterns during early mouse development are related to modes of blood vessel formation and reveal additional sites of hematopoiesis. Blood 90: 2300–2311.
8. Asahara T, Murohara T, Sullivan A, Silver M, van der Zee R, et al. (1997) Isolation of putative progenitor endothelial cells for angiogenesis. Science 275: 964–967.
9. Nonaka-Sarukawa M, Yamamoto K, Aoki H, Nishimura Y, Tomizawa H, et al. (2007) Circulating endothelial progenitor cells in congestive heart failure. Int J Cardiol 119: 344–348.
10. Ott I, Keller U, Knoedler M, Gotze KS, Doss K, et al. (2005) Endothelial-like cells expanded from CD34+ blood cells improve left ventricular function after experimental myocardial infarction. FASEB J 19: 992–994.
11. Segal MS, Shah R, Afzal A, Perrault CM, Chang K, et al. (2006) Nitric oxide cytoskeletal-induced alterations reverse the endothelial progenitor cell migratory defect associated with diabetes. Diabetes 55: 102–109.
12. Shintani S, Kusano K, Ii M, Iwakura A, Heyd L, et al. (2006) Synergistic effect of combined intramyocardial CD34+ cells and VEGF2 gene therapy after MI. Nat Clin Pract Cardiovasc Med 3(Suppl 1): S123–128.
13. Ciarrocchi A, Jankovic V, Shaked Y, Nolan DJ, Mittal V, et al. (2007) Id1 restrains p21 expression to control endothelial progenitor cell formation. PLoS One 2: e1338.
14. Jackson KA, Majka SM, Wang H, Pocius J, Hartley CJ, et al. (2001) Regeneration of ischemic cardiac muscle and vascular endothelium by adult stem cells. J Clin Invest 107: 1395–1402.
15. Kwon SM, Eguchi M, Wada M, Iwami Y, Hozumi K, et al. (2008) Specific Jagged-1 signal from bone marrow microenvironment is required for endothelial progenitor cell development for neovascularization. Circulation 118: 157–165.
16. Kwon SM, Suzuki T, Kawamoto A, Ii M, Eguchi M, et al. (2009) Pivotal role of lnk adaptor protein in endothelial progenitor cell biology for vascular regeneration. Circ Res 104: 969–977.
17. Cheng XW, Kuzuya M, Nakamura K, Maeda K, Tsuzuki M, et al. (2007) Mechanisms underlying the impairment of ischemia-induced neovascularization in matrix metalloproteinase 2-deficient mice. Circ Res 100: 904–913.
18. Lee SP, Youn SW, Cho HJ, Li L, Kim TY, et al. (2006) Integrin-linked kinase, a hypoxia-responsive molecule, controls postnatal vasculogenesis by recruitment of endothelial progenitor cells to ischemic tissue. Circulation 114: 150–159.
19. Chavakis E, Aicher A, Heeschen C, Sasaki K, Kaiser R, et al. (2005) Role of beta2-integrins for homing and neovascularization capacity of endothelial progenitor cells. J Exp Med 201: 63–72.
20. Carmona G, Chavakis E, Koehl U, Zeiher AM, Dimmeler S (2008) Activation of Epac stimulates integrin-dependent homing of progenitor cells. Blood 111: 2640–2646.
21. Walter DH, Haendeler J, Reinhold J, Rochwalsky U, Seeger F, et al. (2005) Impaired CXCR4 signaling contributes to the reduced neovascularization capacity of endothelial progenitor cells from patients with coronary artery disease. Circ Res 97: 1142–1151.
22. Kamei N, Kwon SM, Alev C, Ishikawa M, Yokoyama A, et al. (2010) Lnk deletion reinforces the function of bone marrow progenitors in promoting neovascularization and astrogliosis following spinal cord injury. Stem Cells 28: 365–375.
23. Yamamoto K, Takahashi T, Asahara T, Ohura N, Sokabe T, et al. (2003) Proliferation, differentiation, and tube formation by endothelial progenitor cells in response to shear stress. J Appl Physiol 95: 2081–2088.
24. Eguchi M, Masuda H, Kwon S, Shirakura K, Shizuno T, et al. (2008) Lesion-targeted thrombopoietin potentiates vasculogenesis by enhancing motility and enlivenment of transplanted endothelial progenitor cells via activation of Akt/mTOR/p70S6kinase signaling pathway. J Mol Cell Cardiol 45: 661–669.
25. Jin H, Aiyer A, Su J, Borgstrom P, Stupack D, et al. (2006) A homing mechanism for bone marrow-derived progenitor cell recruitment to the neovasculature. J Clin Invest 116: 652–662.
26. Ceradini DJ, Kulkarni AR, Callaghan MJ, Tepper OM, Bastidas N, et al. (2004) Progenitor cell trafficking is regulated by hypoxic gradients through HIF-1 induction of SDF-1. Nat Med 10: 858–864.
27. Kimura T, Boehmler AM, Seitz G, Kuci S, Wiesner T, et al. (2004) The sphingosine 1-phosphate receptor agonist FTY720 supports CXCR4-dependent migration and bone marrow homing of human CD34+ progenitor cells. Blood 103: 4478–4486.
28. Yamaguchi J, Kusano KF, Masuo O, Kawamoto A, Silver M, et al. (2003) Stromal cell-derived factor-1 effects on ex vivo expanded endothelial progenitor cell recruitment for ischemic neovascularization. Circulation 107: 1322–1328.
29. Morrison SJ, Weissman IL (1994) The long-term repopulating subset of hematopoietic stem cells is deterministic and isolatable by phenotype. Immunity 1: 661–673.
30. Bailey AS, Jiang S, Afentoulis M, Baumann CI, Schroeder DA, et al. (2004) Transplanted adult hematopoietic stems cells differentiate into functional endothelial cells. Blood 103: 13–19.
31. Grant MB, May WS, Caballero S, Brown GA, Guthrie SM, et al. (2002) Adult hematopoietic stem cells provide functional hemangioblast activity during retinal neovascularization. Nat Med 8: 607–612.
32. Sebzda E, Hibbard C, Sweeney S, Abtahian F, Bezman N, et al. (2006) Syk and Slp-76 mutant mice reveal a cell-autonomous hematopoietic cell contribution to vascular development. Dev Cell 11: 349–361.
33. Kim H, Cho HJ, Kim SW, Liu B, Choi YJ, et al. (2010) CD31+ Cells Represent Highly Angiogenic and Vasculogenic Cells in Bone Marrow: Novel Role of Nonendothelial CD31+ Cells in Neovascularization and Their Therapeutic Effects on Ischemic Vascular Disease. Circ Res 107: 602–614.
34. Balsam LB, Wagers AJ, Christensen JL, Kofidis T, Weissman IL, et al. (2004) Haematopoietic stem cells adopt mature haematopoietic fates in ischaemic myocardium. Nature 428: 668–673.
35. Murry CE, Soonpaa MH, Reinecke H, Nakajima H, Nakajima HO, et al. (2004) Haematopoietic stem cells do not transdifferentiate into cardiac myocytes in myocardial infarcts. Nature 428: 664–668.
36. Iwasaki H, Kawamoto A, Ishikawa M, Oyamada A, Nakamori S, et al. (2006) Dose-dependent contribution of CD34-positive cell transplantation to concur-

rent vasculogenesis and cardiomyogenesis for functional regenerative recovery after myocardial infarction. Circulation 113: 1311–1325.
37. Timmermans F, Plum J, Yoder MC, Ingram DA, Vandekerckhove B, et al. (2009) Endothelial progenitor cells: identity defined? J Cell Mol Med 13: 87–102.
38. Tanaka R, Wada M, Kwon SM, Masuda H, Carr J, et al. (2008) The effects of flap ischemia on normal and diabetic progenitor cell function. Plast Reconstr Surg 121: 1929–1942.
39. Dimmeler S, Aicher A, Vasa M, Mildner-Rihm C, Adler K, et al. (2001) HMG-CoA reductase inhibitors (statins) increase endothelial progenitor cells via the PI 3-kinase/Akt pathway. J Clin Invest 108: 391–397.
40. Kalka C, Masuda H, Takahashi T, Kalka-Moll WM, Silver M, et al. (2000) Transplantation of ex vivo expanded endothelial progenitor cells for therapeutic neovascularization. Proc Natl Acad Sci U S A 97: 3422–3427.
41. Vasa M, Fichtlscherer S, Aicher A, Adler K, Urbich C, et al. (2001) Number and migratory activity of circulating endothelial progenitor cells inversely correlate with risk factors for coronary artery disease. Circ Res 89: E1–7.
42. De Palma M, Venneri MA, Roca C, Naldini L (2003) Targeting exogenous genes to tumor angiogenesis by transplantation of genetically modified hematopoietic stem cells. Nat Med 9: 789–795.
43. Gothert JR, Gustin SE, van Eekelen JA, Schmidt U, Hall MA, et al. (2004) Genetically tagging endothelial cells in vivo: bone marrow-derived cells do not contribute to tumor endothelium. Blood 104: 1769–1777.
44. Timmermans F, Van Hauwermeiren F, De Smedt M, Raedt R, Plasschaert F, et al. (2007) Endothelial outgrowth cells are not derived from CD133+ cells or CD45+ hematopoietic precursors. Arterioscler Thromb Vasc Biol 27: 1572–1579.
45. Case J, Mead LE, Bessler WK, Prater D, White HA, et al. (2007) Human CD34+AC133+VEGFR-2+ cells are not endothelial progenitor cells but distinct, primitive hematopoietic progenitors. Exp Hematol 35: 1109–1118.
46. Asai J, Takenaka H, Kusano KF, Ii M, Luedemann C, et al. (2006) Topical sonic hedgehog gene therapy accelerates wound healing in diabetes by enhancing endothelial progenitor cell-mediated microvascular remodeling. Circulation 113: 2413–2424.
47. Ii M, Nishimura H, Iwakura A, Wecker A, Eaton E, et al. (2005) Endothelial progenitor cells are rapidly recruited to myocardium and mediate protective effect of ischemic preconditioning via "imported" nitric oxide synthase activity. Circulation 111: 1114–1120.

Surg Today (2011) 41:1029–1036
DOI 10.1007/s00595-010-4526-3

SURGERY TODAY

Original Article

Clinical Impact of Combined Transplantation of Autologous Skeletal Myoblasts and Bone Marrow Mononuclear Cells in Patients with Severely Deteriorated Ischemic Cardiomyopathy

TOMOYUKI FUJITA[1], TAICHI SAKAGUCHI[1], SIGERU MIYAGAWA[1], ATSUHIRO SAITO[2], NAOSUMI SEKIYA[1], HIRONORI IZUTANI[1], and YOSHIKI SAWA[1,2]

[1] Division of Cardiovascular Surgery, Department of Surgery, Osaka University, Graduate School of Medicine, 2-2 Yamadaoka, Suita, Osaka 565-0871, Japan
[2] Medical Center for Translational Research, Osaka University Hospital, Osaka, Japan

Abstract

Purpose. Simultaneous injection of autologous bone marrow cells and skeletal myoblasts has been demonstrated to improve cardiac function in animal models. We evaluated the potential application of this combination cell therapy in patients with severe ischemic cardiomyopathy who required left ventricular assist device (LVAD) implantation.

Methods. Four patients (age range, 43–69 years) who required LVAD implantation due to severe ischemic cardiomyopathy were studied. Skeletal myoblasts were obtained from the thigh, while bone marrow mononuclear cells were collected and purified at the time of the operation. These cells were directly injected in a serial manner into the damaged myocardium.

Results. No fatal arrhythmias or major complications were observed. The number of injected skeletal myoblasts ranged from 2.7×10^7 to 3.0×10^8, and their purity ranged from 25% to 96%. Two patients showed decreased brain natriuretic peptide levels and echocardiographic improvements in the transplanted areas, as well as increased perfusion revealed by $H_2{}^{15}O$ positron emission tomography, of whom one was successfully weaned from LVAD. Histological findings at autopsy of the other patient showed a small amount of skeletal muscle in the injected area. Only marginal improvements were observed in the other two patients.

Conclusions. Combined cell transplantation is feasible for patients with severe ischemic cardiomyopathy, and functional recovery is anticipated in selected patients.

Key words Cell transplantation · Device · Heart failure · Cardiomyopathy

Reprint requests to: Y. Sawa (address 1)
Received: June 29, 2010 / Accepted: December 8, 2010

Introduction

Regenerative medicine is expected to provide an alternative treatment for end-stage heart failure, by providing methods to regenerate heart muscle and recover cardiac function in affected patients. Bone marrow stem cells (BMSCs) have been used in a number of clinical trials, as they are expected to differentiate into cardiac muscle or capillary cells to regenerate cardiac tissue.[1–4] The cells seem to be useful to restore lost functionality due to acute myocardial infarction by improving ejection fraction (EF) and exercise tolerance, or reducing infarcted areas through angiogenesis.[1–4] However, no clinical studies have shown BMSCs to be useful for chronic heart failure.

On the other hand, skeletal muscle has shown a capacity for self repair, because of a resident population of proliferative muscle cells known as myoblasts.[5] Once activated, skeletal myoblasts can form new muscle to restore lost functionality. Menasché et al. were the first to use cultured skeletal myoblasts in a study of ten patients with ischemic cardiomyopathy,[6] in whom they transplanted cells by direct injection to infarcted areas. Those skeletal myoblast injections in combination with surgical treatments increased the EF by improving local myocardial thickening, and consequently, improved their New York Heart Association (NYHA) classification. However, four of their patients required treatment with an internal cardioventricular defibrillator (ICD) due to ventricular tachycardia. Although a large randomized study (MAGIC trial) performed thereafter did not find significant improvements in cardiac function or postoperative arrhythmic events, high-dose myoblast transplantation showed the capacity to improve diastolic function through paracrine effects.[7] Furthermore, Dib et al. found survival and engraftment of transplanted myoblasts and improvement of clinical cardiac data, which suggested the feasibility and safety of autologous myoblast transplantation.[8]

Our preclinical data, obtained with a canine chronic myocardial infarction model, demonstrated that a combination of autologous skeletal myoblasts and BMSCs provided better cardiac performance than did either cell type alone, because of their induction of both myogenesis and angiogenesis.[9] Ott et al. also suggested that combination cell therapy may be clinically relevant by merging the beneficial effects of each cell line, based on data obtained from a rat model.[10] The first clinical case also confirmed the relevance of combined cell therapy;[11] therefore, the objectives of the present study were to assess the safety and feasibility of combination cell therapy in a clinical setting.

All patients recruited for the present study had end-stage heart failure due to ischemic cardiomyopathy (ICM) requiring a left ventricular assist device (LVAD). This patient group was considered unlikely to recover their cardiac function by mechanical unloading.[12] Cell transplantation was the only procedure performed, and cardiac function was assessed before and after the operation.

Patients and Methods

Patient Selection

Patients were considered eligible if all of the following criteria were met: (1) age between 18 and 70 years old, (2) a history of myocardial infarction and subsequent alteration of left ventricular function, and (3) end-stage heart failure with symptoms of NYHA functional class IV with intravenous catecholamine, with or without optimal contemporary medical management, including angiotensin-converting enzyme inhibitors and β-blockers requiring an LVAD, or an LVAD already being utilized. Regardless of the indications for heart transplantation, the LVAD was implanted into the patients who met the above criteria and were suggested not to survive without LVAD implantation due to end-stage heart failure. The major exclusion criteria were peripheral muscular dystrophy, malignancy, pregnancy, alcoholism, positive serologic test results for human immunodeficiency virus, hepatitis, human T lymphotropic virus type 1, and syphilis. The study was approved by the Ethical Committee and Internal Review Board (IRB) of Osaka University, and informed consent was obtained from each participant.

Study Registration

This study was registered in the UMIN Clinical Trials Registry (UMIN-CTR) and the registration number is UMIN000001859. The date of protocol fixation was April 1, 2004, and first patient was enrolled on July 5, 2004.

LVAD Implantation and Cell Transplantation

Prior to cell transplantation, all patients underwent implantation of an extracorporeal pneumatic LVAD (Toyobo, Tokyo, Japan) through a median sternotomy. The interval between LVAD implantation and cell transplantation was 155 ± 86 days (range 101–284 days). Cell transplantation was performed by injection through a left thoracotomy with a 1-ml syringe that contained myoblasts or bone marrow mononuclear cells (BM-MNCs). Prior to the injection, cultured autologous myoblasts and freshly extracted autologous BM-MNCs were separately suspended in 3 ml of Dulbecco's modified Eagle's medium solution and separated into 10 1-ml syringes for each cell type. The cells were injected into the intramyocardial area with a 26-gauge needle, anterior to the lateral and posterior myocardium as far as possible. Maximum technical care was taken to avoid loss of cells.

Myoblast Isolation Procedure

For each patient, a muscle biopsy specimen was obtained from the tibialis anterior and/or medial vastus muscle (weight range, 3.8–22 g), then washed in ice-cold normal saline solution. Each muscle specimen was immediately packed in a resealable container filled with preservation medium and transferred to the Cell Processing Center (Medical Center for Translational Research, Osaka University Hospital), where the myoblasts were isolated and cultured according to the method of Dib et al.[8] The cell culture was continued until an adequate number of cells (>300 × 10^6) was obtained. Purity was confirmed, and cell counting was performed using a fluorescence-activated cell sorter (FACS) analysis with a CD56 antibody (BD, Rockville, MD, USA). Once the target number of cells was reached, the cultured cells were frozen in liquid nitrogen until transplantation. The interval between myoblast harvesting and cell transplantation was 69 ± 45 days (range 41–136 days). These cell processing procedures were safely performed following the ordinance of Ministry of Health, Labour and Welfare of Japan regarding good manufacturing practices, even though it was not mandatory.

Extraction of BM-MNCs

A total of 200–300 million bone marrow (BM) cells were aspirated from the ileum with a BM harvest needle just before cell transplantation. Bone marrow-MNCs were then sorted using a CS3000-Plus blood-cell separator (Baxter, Deerfield, IL, USA) according to the method reported by Tateishi-Yuyama et al.[13] Bone marrow aspiration was performed until more than 100 × 10^6 cells were obtained.

RhythmM onitoring

All patients were hospitalized during this study and monitored by 24-h telemetry, and Holter electrocardiograms (ECG) were obtained at 1, 2, 3, and 6 months postoperatively.

Assessment of Cardiac Function

Cardiac function was assessed by measuring the serum brain natriuretic peptide (BNP) levels, while the left ventricular ejection fraction (LVEF) was determined by two-dimensional echocardiography. While the patient was supported by LVAD, LVEF was measured using the LVAD off-study technique.[12]

Color Kinesis

Diastolic color kinesis images performed 1 month after cell transplantation were obtained from the left ventricle in the mid-papillary short-axis view. The timing of color encoding was set to begin at the first frame, in which outward endocardial motion was noted, and its duration was set to the maximum value (26 frames). The regional fraction area change was considered to be the regional incremental fraction area that changed during diastole in regard of the percentage of regional end-diastolic area in the short-axis view. The color kinesis diastolic index (CK-DI) was defined as the left ventricular (LV) segmental filling fraction during the first 30% of the diastolic filling period, and was used to assess regional LV active relaxation.[14]

Histopathology

Histopathology samples were obtained from the LV apex at the time of LVAD implantation or from an anterolateral lesion at the site of transplantation. Standard histological examinations were performed with hematoxylin–eosin staining, with Masson's trichrome staining used to visualize fibrosis. Immunostaining of the fast-isoform myosin heavy chain (Sigma, St. Louis, MO, USA) was performed to reveal transplanted myoblasts at the site of transplantation. Immunohistochemical staining using factor VIII-related antigen (DAKO EPOS Anti-Human Von Willebrand Factor/HRP; DAKO, Glostrup, Denmark) was performed to visualize vascular density.

Results

Patients

Four patients met the criteria for enrollment in this study, and underwent LVAD implantation and cell transplantation. Patient demographics are shown in Table 1. Their age ranged from 43 to 69 years old. The interval from myocardial infarction and cell transplantation ranged from 4 to 9 months. All patients had end-stage heart failure with symptoms of NYHA functional class IV and required Toyobo extracorporeal LVAD implantation prior to cell transplantation, and none of them showed functional recovery between the LVAD implantation and cell transplantation. The two younger patients were considered to be eligible for heart transplantation, but the other two were not, due to their advanced age.

Cell Culture

There were no serious complications related to the muscle biopsy procedures and no problems encountered during cell culturing at the Cell Processing Center. In addition, there was no bacterial or fungal contamination, as determined by US Pharmacopeia sterility, mycoplasma testing, and by examining the levels of endotoxin in the culture media. Cell cultures were terminated when the cell count reached more than 300×10^6 cells. The culture periods ranged from 20 to 23 days. The viability of cells ranged from 93% to 98% at the time of cell transplantation. However, the purity was different in each patient, thus the actual numbers of surviving myoblasts injected were 138×10^6 and 248×10^6 in the two younger patients (patients 1 and 2), respectively, and 77×10^6 and 58×10^6 in the two older patients (patients 3 and 4), respectively. On the other hand, an adequate number (more than 200×10^6 cells) of BM-MNCs was obtained from each patient.

Adverse Events

No deaths or arrhythmias occurred during the cell injections, and minimal bleeding was observed from the injection sites. All patients were in stable condition postoperatively with LVAD support. There was no sustained ventricular tachycardia (VT) or ventricular fibrillation (Vf) recorded postoperatively by 24-h electrocardiogram telemetry. The Holter ECG revealed that only 141 ± 177 ventricular premature beats (VPBs)/day were recorded and 1.8 ± 2.5 couplets/day were recorded. No VTs or Vfs were detected. Although the LVAD was successfully removed from patient 1 at 360 days after cell transplantation, he died due to recurrence of heart failure after refusing reintroduction of LVAD at 351 days after LVAD removal (Table 2). In addition, another patient died due to sepsis at 346 days after cell transplantation, and two from cancer at 211 days and 379 days after cell transplantation, respectively. There were no major transplantation-related adverse events.

Table 1. Patients' demographics

Patient	Age (years)	Myocardial infarction: Age (months)	Myocardial infarction: Location	NYHA Class	Mechanical support	Pre-Tx EF (%)	Culture period (days)	Cell transplantation: No. of cells injected ($\times 10^6$)	Cell transplantation: Viability of cells (%)	Cell transplantation: Purity of myoblasts (%)	Cell transplantation: No. of myoblasts injected ($\times 10^6$)	Cell transplantation: No. of bone marrow mononuclear cells ($\times 10^6$)
1	53	7	LMT	IV	LVAD	22	22	300	98	47	138	200
2	43	4	LMT	IV	LVAD	17	20	300	93	89	248	300
3	69	5	LMT	IV	LVAD	10	23	300	95	27	77	240
4	67	9	LMT	IV	LVAD	37	20	300	96	20	58	250

LMT, left main trunk; NYHA, New York Heart Association; LVAD, left ventricular assist device; Tx, transplantation

Functional Assessment

Left ventricular ejection fraction was improved in three patients, and the patients who received a larger number of cultured myoblasts (patients 1 and 2) showed more than 10% improvement (Fig. 1). These improvements were detected at the 1-month follow-up examination and were amplified at 6 months after the procedure in patient 2 and at 1 year in patient 1, who showed 21% improvement at the 1-year follow-up examination, which led us to wean him off the LVAD. Improvement in EF was marginal in patient 3, while patient 4 showed no improvement in the LVEF.

Three patients (1, 2, and 3) underwent color kinesis analysis. The mean CK-DI was improved from 33% to 53% in patient 1 and from 23% to 41% in patient 2 (Fig. 2). In detail, the regional improvements in CK-DI were remarkable in the lateral, anterior, and posterior regions where cell transplantation was performed, while other areas also showed improvement in regional LV active relaxation in those patients. On the other hand, patient 3 did not show any improvement of diastolic function, even in the transplanted area. Patients 1 and 2 also showed remarkable decreases in BNP levels after the operation (Fig. 3), whereas patients 3 and 4 did not. When data for LVEF, diastolic function, and BNP level were combined, patients 1 and 2 showed improvement in cardiac function after cell transplantation, whereas patients 3 and 4 did not.

Histological Analysis

Post-transplantation biopsies were performed in 3 patients, at the time of LVAD removal in patient 1, and at autopsy in patients 2 and 4, while the family of patient 3 refused the autopsy procedure. Immunostaining of the fast-isoform myosin heavy chain detected a very small number of myoblasts in patient 2 (Fig. 4A), and the positive control confirmed that the stained cells were of skeletal muscle origin (Fig. 4B). No myoblasts were detected in patients 1 and 4. In patient 2, factor VIII immunostaining showed that the microvasculature network was increased following the operation (Fig. 5A) as compared to before transplantation (Fig. 5B). The preoperative biopsy specimen obtained from patient 1 showed global infarction and tissue damage (Fig. 5C), while that obtained postoperatively from the transplanted area at the time of LVAD removal showed well-settled muscle cells (Fig. 5D). On the other hand, the preoperative biopsy specimen obtained from patient 4 showed severe ischemic changes and a necrotic myocardium (Fig. 5E), and that obtained postoperatively at autopsy showed scarring and very few surviving cells (Fig. 5F). Therefore, postoperative biopsy results supported other evidence showing that patient 1 had recovered cardiac function, while patient 4 did not.

Table 2. Patients' outcomes after transplantation

Patient	Sustained VT or Vf	LVAD removal	Days after transplantation	Current status	Survival (days)	Cause of death
1	No	Yes	360	Deceased	711	Heart failure
2	No	No	—	Deceased	345	Sepsis
3	No	No	—	Deceased	221	Pharyngeal cancer
4	No	No	—	Deceased	360	Bladder cancer

VT, ventricular tachycardia; Vf, ventricular fibrillation; LVAD, left ventricular assist device

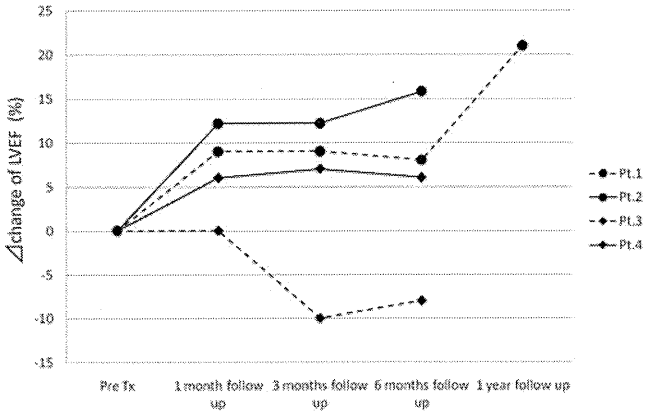

Fig. 1. Changes in baseline left ventricular ejection fraction (*LVEF*) at 1 month, 3 months, 6 months, and 1 year after the procedure. Ejection fractions were obtained at the time of left ventricular assist device (LVAD) implantation. *Pt*, patient; *Pre Tx*, before transplantation

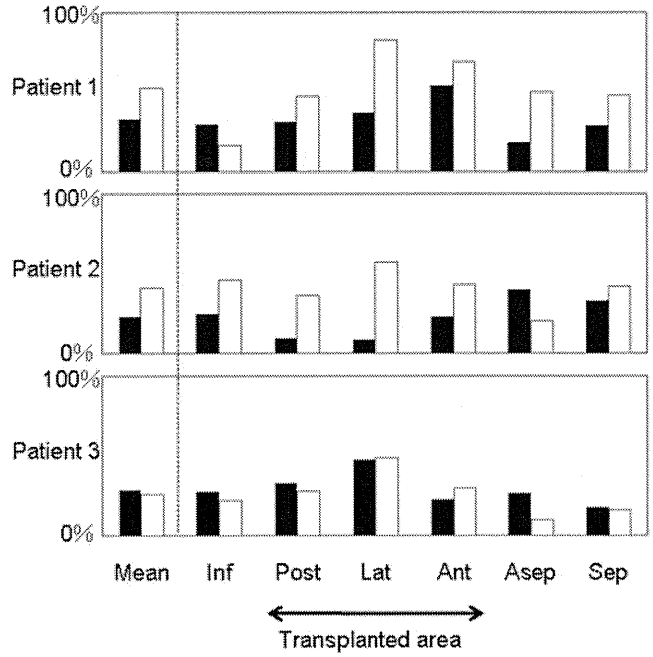

Fig. 2. Changes in diastolic color kinesis index (CK-DI) between the preoperative baseline (*black bars*) and the postoperative follow-up (*white bars*) examinations. CK-DI expresses the expansion speed of the left ventricle during the diastolic phase, which implies LV diastolic function. The left ventricle was divided into six segments as defined in the American Society of Echocardiography guidelines. Cell transplantation was performed lateral to the posterior and anterior regions

Study Limitations

Only four patients were enrolled in this study, therefore the data were insufficient to evaluate their statistical significance. Second, analysis of the effects of cell transplantation alone was difficult, because the mechanical unloading effect of LVAD may have been significant.

Discussion

This study is the human trial to show the possibility of combination therapy with autologous bone marrow cells and cultured myoblasts. Bone marrow stem cells are reported to have a high capacity for angiogenesis,[15] as well as the potential to be mobilized and differentiate into cardiomyocytes and induce new capillary formation and proliferation of the preexisting vasculature network.[16] Although Orlic et al. suggested that c-kit positive cells could generate de novo myocardium,[17] Balsam et al. and Murry et al. reported different conclusions.[18,19] On the other hand, experiments with skeletal myoblasts have shown that they can differentiate into myotubes and improve postinfarction cardiac function.[20,21] Thus, is reasonable to consider that implanta-

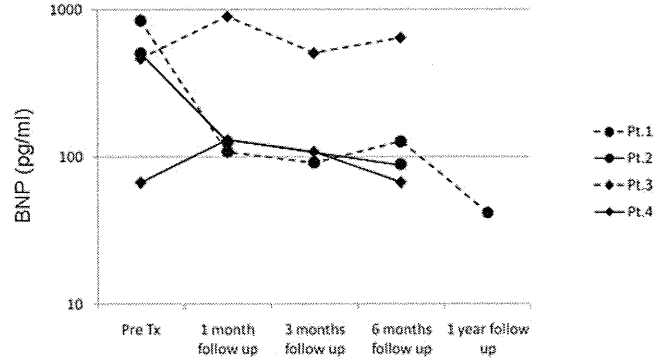

Fig. 3. Changes in baseline brain natriuretic peptide (*BNP*) levels at 1 month, 3 months, 6 months, and 1 year after the procedure

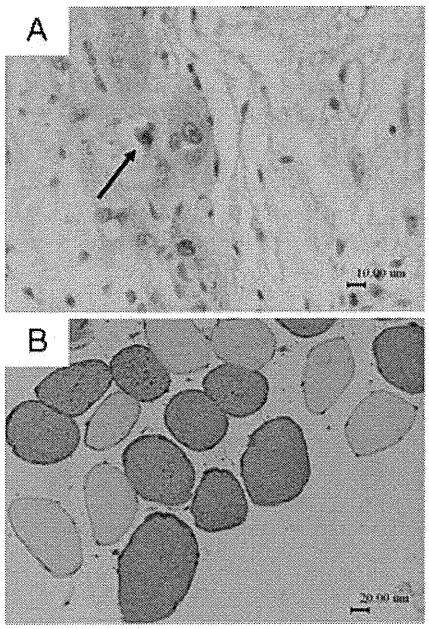

Fig. 4. **A** Biopsy specimen obtained from patient 2 from the transplanted area at the time of autopsy (fast-isoform myosin heavy chain staining). **B** Skeletal muscle tissue was used as a positive control

tion of contractile cells into areas of postinfarction scarring could functionally rejuvenate those areas.

In the present study, two of the patients had EF improvement greater than 10%, as well as improved diastolic function in both transplanted and nontransplanted areas, and decreased BNP levels after cell transplantation. Patient 2 showed a slightly increased vasculature network, although very few myoblasts were noted (Fig. 5A and B), as described in our previous case report,[11] while patient 1 did not show any engrafted myoblasts postoperatively. Therefore, as experimental studies have shown that a very low number of cells (in the range of 1%) are engrafted within a few weeks after transplantation, paracrine effects, rather than myogenesis, are considered to be the crucial mechanisms involved in cell therapy, in which transplanted cells may trigger an endogenous pathway to activate and/or protect existing cardiomyocytes by angiogenesis and cytokine delivery.[22] Although these effects may be conferred by BMSCs solely, additional beneficial effects of skeletal myoblasts were also expected based on animal experiments.[9] Moreover, the improvement in global diastolic function in the present patients may also be explained by paracrine effects, as Farahmand et al.

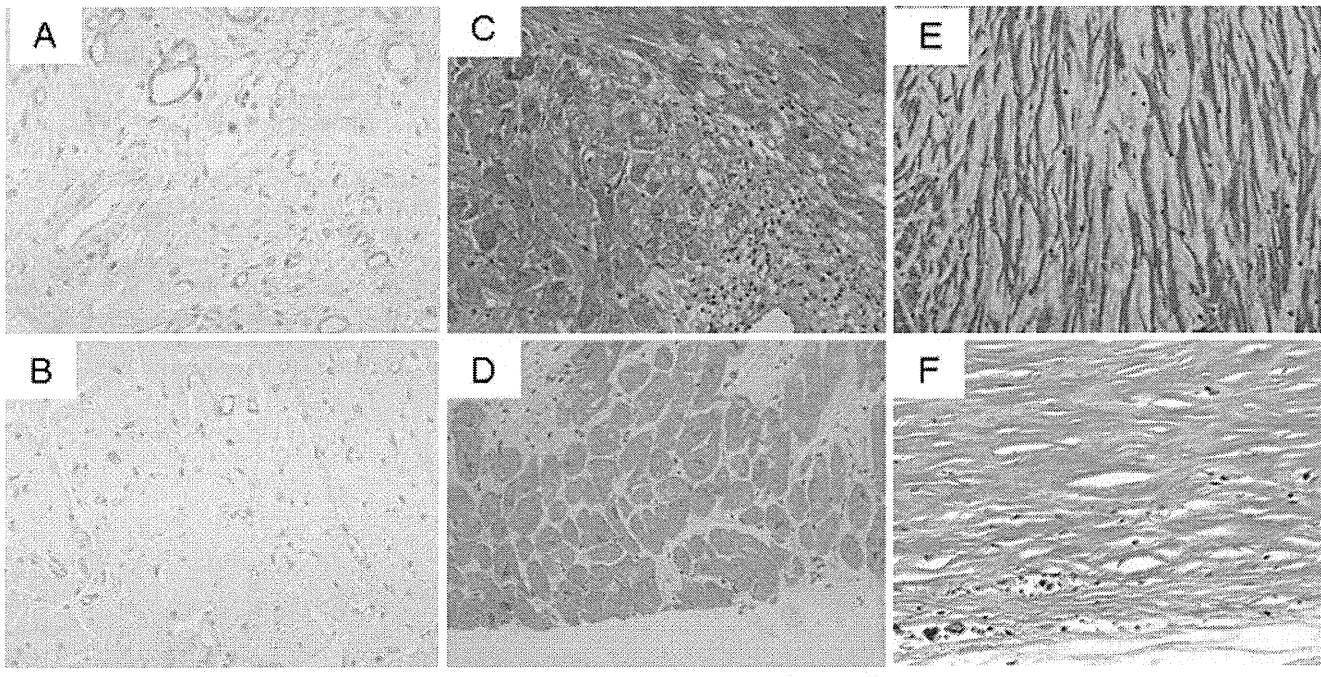

Fig. 5A–F. Histological results. **A** Biopsy specimen obtained from the transplanted area in patient 2 at the time of autopsy showing rich vasculature. **B** Poor vasculature in a tissue specimen from the LV apical core removed at the time of LVAD implantation. Both specimens **A** and **B** were stained using a Factor VIII antibody. **C** Surgical specimen obtained from the LV lateral wall in patient 1 at the time of LVAD implantation showing acute myocardial infarction. **D** Biopsy specimen obtained from the same site as **C** at the time of LVAD removal, showing well-settled muscle tissues. **E** Surgical specimen obtained from the LV apex of patient 4 at the time of LVAD implantation, showing few surviving cells as compared to the biopsy specimen from the same site obtained at autopsy from patient 1 (shown in **D**). The specimens shown in **C**, **D**, **E**, and **F** were stained with hematoxylin–eosin using a customary technique

reported that skeletal myoblasts prevented ventricular dilation and preserved the matrix architecture in a remote region through paracrine effects.[23] These mechanisms require further elucidation in future studies.

In the MAGIC trial only the high-dose group (8.0×10^8 cells) showed beneficial effects on improving diastolic function,[7] while cardiac reverse remodeling occurred in a dose-dependent manner in a rat myocardial infarction model.[24] While the number of injected BMSCs was fairly consistent among the four patients in our study, this was not the case for the myoblasts, the number of which dramatically varied from 58 to 248 million. It is currently unclear as to what number of cells is optimal for such treatment, and it is technically difficult to maximize the number and purity of myoblasts in elderly patients, making it difficult to interpret the outcomes. Therefore, the cell ratio may be critical, and an age limit should be considered for myoblast therapy.

The preoperative specimen from patient 4 obtained from the target area showed scar-like tissue, in which a low number of cells was found (Fig. 5E). The postoperative biopsy specimen showed similar findings (Fig. 5F), in contrast to the postoperative specimen obtained from patient 1 (Fig. 5D). Therefore, we consider that a minimum number of pre-existing cells is needed for cell therapy to provide paracrine effects, such as repair and reinforcement.

Concerning arrhythmia, we did not detect a lethal arrhythmia during the entire period of clinical study (6 months). Although cell transplantation by injection was suspected to cause lethal arrhythmias by re-entry circuit formation, no sustained VTs were identified during 24-h telemetry, and no VTs longer than triplets were recorded by the Holter ECG. We speculated that the amount of implanted myocytes in this study might not have been sufficient to confer electrical activity to cause an arrhythmia, and the mechanical unloading provided by the LVAD may also have prevented an arrhythmia.

In summary, this study suggested that combined cell therapy is feasible, but a large-scale study without LVAD is required to examine the effects of cell transplantation alone and to identify patients who are likely to respond to this therapy.

References

1. Meyer GP, Wollert KC, Lotz J, Steffens J, Lippolt P, Fichtner S, et al. Intracoronary bone marrow cell transfer after myocardial infarction: eighteen months' follow-up data from the randomized, controlled BOOST (BOne marrOw transfer to enhance ST-elevation infarct regeneration) trial. Circulation 2006;113:1287–94.
2. Lunde K, Solheim S, Aakhus S, Arnesen H, Moum T, Abdelnoor M, et al. Exercise capacity and quality of life after intracoronary injection of autologous mononuclear bone marrow cells in acute myocardial infarction: results from the Autologous Stem cell Transplantation in Acute Myocardial Infarction (ASTAMI) randomized controlled trial. Am Heart J 2007;154:710.e1–8.
3. Schächinger V, Assmus B, Britten MB, Honold J, Lehmann R, Teupe C, et al. Transplantation of progenitor cells and regeneration enhancement in acute myocardial infarction: final one-year results of the TOPCARE-AMI Trial. J Am Coll Cardiol 2004;44: 1690–9.
4. Erbs S, Linke A, Schächinger V, Assmus B, Thiele H, Diederich KW, et al. Restoration of microvascular function in the infarct-related artery by intracoronary transplantation of bone marrow progenitor cells in patients with acute myocardial infarction: the Doppler Substudy of the Reinfusion of Enriched Progenitor Cells and Infarct Remodeling in Acute Myocardial Infarction (REPAIR-AMI) trial. Circulation 2007;116:366–74.
5. Bischoff R. Regeneration of single skeletal muscle fibers in vitro. Anat Rec 1975;182:215–35.
6. Menasché P, Hagège AA, Scorsin M, Pouzet B, Desnos M, Duboc D, et al. Myoblast transplantation for heart failure. Lancet 2001; 357:279–80.
7. Menasché P, Alfieri O, Janssens S, McKenna W, Reichenspurner H, Trinquart L, et al. The Myoblast Autologous Grafting in Ischemic Cardiomyopathy (MAGIC) trial: first randomized placebo-controlled study of myoblast transplantation. Circulation 2008;117(9):1189–200.
8. Dib N, Michler RE, Pagani FD, Wright S, Kereiakes DJ, Lengerich R, et al. Safety and feasibility of autologous myoblast transplantation in patients with ischemic cardiomyopathy: four-year follow-up. Circulation 2005;112(12):1748–55.
9. Memon IA, Sawa Y, Miyagawa S, Taketani S, Matsuda H. Combined autologous cellular cardiomyoplasty with skeletal myoblasts and bone marrow cells in canine hearts for ischemic cardiomyopathy. J Thorac Cardiovasc Surg 2005;130:646–53.
10. Ott HC, Bonaros N, Marksteiner R, Wolf D, Margreiter E, Schachner T, et al. Combined transplantation of skeletal myoblasts and bone marrow stem cells for myocardial repair in rats. Eur J Cardiothorac Surg 2004;25:627–34.
11. Miyagawa S, Matsumiya G, Funatsu T, Yoshitatsu M, Sekiya N, Fukui S, et al. Combined autologous cellular cardiomyoplasty using skeletal myoblasts and bone marrow cells for human ischemic cardiomyopathy with left ventricular assist system implantation: report of a case. Surg Today 2009;39:133–6.
12. Matsumiya G, Monta O, Fukushima N, Sawa Y, Funatsu T, Toda K, et al. Who would be a candidate for bridge to recovery during prolonged mechanical left ventricular support in idiopathic dilated cardiomyopathy? J Thorac Cardiovasc Surg 2005;130: 699–704.
13. Tateishi-Yuyama E, Matsubara H, Murohara T, Ikeda U, Shintani S, Masaki H, et al. Therapeutic Angiogenesis using Cell Transplantation (TACT) Study Investigators. Therapeutic angiogenesis for patients with limb ischaemia by autologous transplantation of bone-marrow cells: a pilot study and a randomised controlled trial. Lancet 2002;360:427–35.
14. Mor-Avi V, Vignon P, Koch R, Weinert L, Garcia MJ, Spencer KT, et al. Segmental analysis of color kinesis images: new method for quantification of the magnitude and timing of endocardial motion during left ventricular systole and diastole. Circulation 1997;95: 2082–97.
15. Blau HM, Brazelton TR, Weimann JM. The evolving concept of a stem cell: entity or function? Cell 2001;105:829–41.
16. Krause DS, Theise ND, Collector MI, Henegariu O, Hwang S, Gardner R, et al. Multi-organ, multi-lineage engraftment by a single bone marrow-derived stem cell. Cell 2001;105:369–77.
17. Orlic D, Kajstura J, Chimenti S, Bodine DM, Leri A, Anversa P. Bone marrow cells regenerate infarcted myocardium. Nature 2001;410:701–5.
18. Murry CE, Soonpaa MH, Reinecke H, Nakajima H, Nakajima HO, Rubart M, et al. Haematopoietic stem cells do not transdifferentiate into cardiac myocytes in myocardial infarcts. Nature 2004;428:664–8.